ONLINE SUPPLEMENT

Use of hydraulic radius to estimate the permeability of coarse-grained materials using a new geodatabase

Shuyin Feng, Daniel Barreto, Emőke Imre, Erdin Ibraim & Paul J. Vardanega

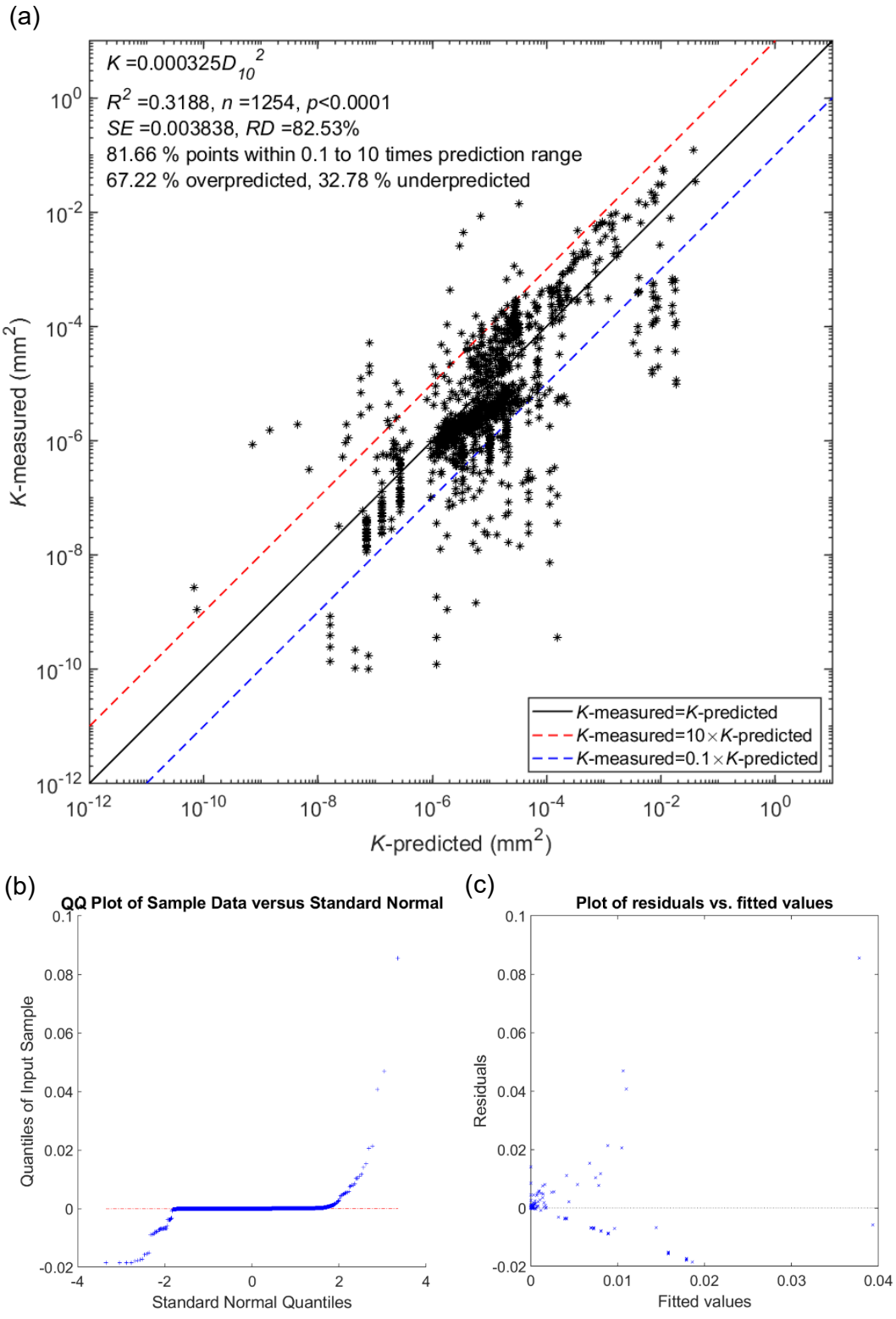

Figure S1. Regression result using a Hazen (1893, 1895, 1911) style model: calibrated using the full database (plots adapted from Feng 2022)

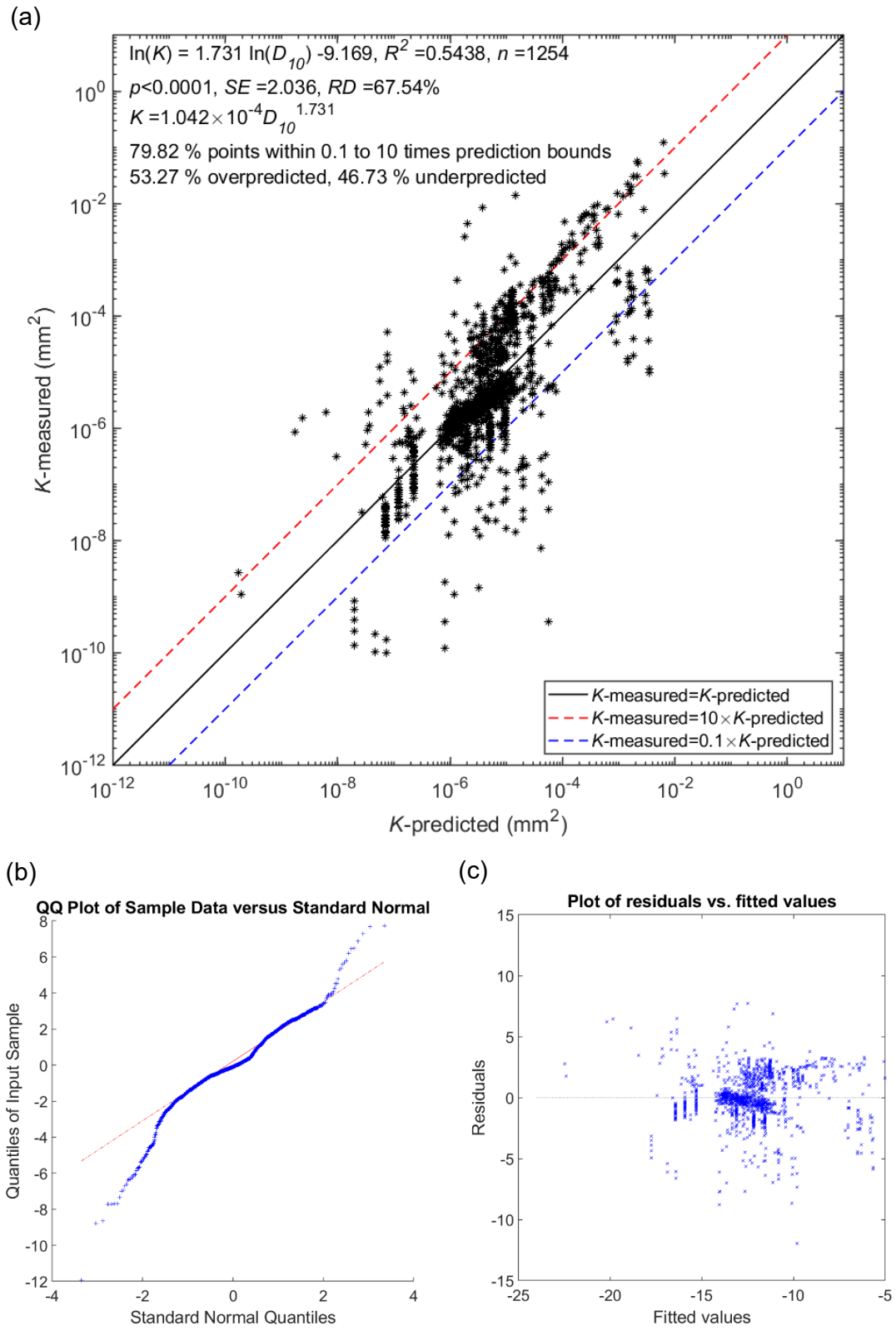

Figure S2. Regression result using a Shepherd (1989) style model: calibrated using the full database (plots adapted from Feng 2022)

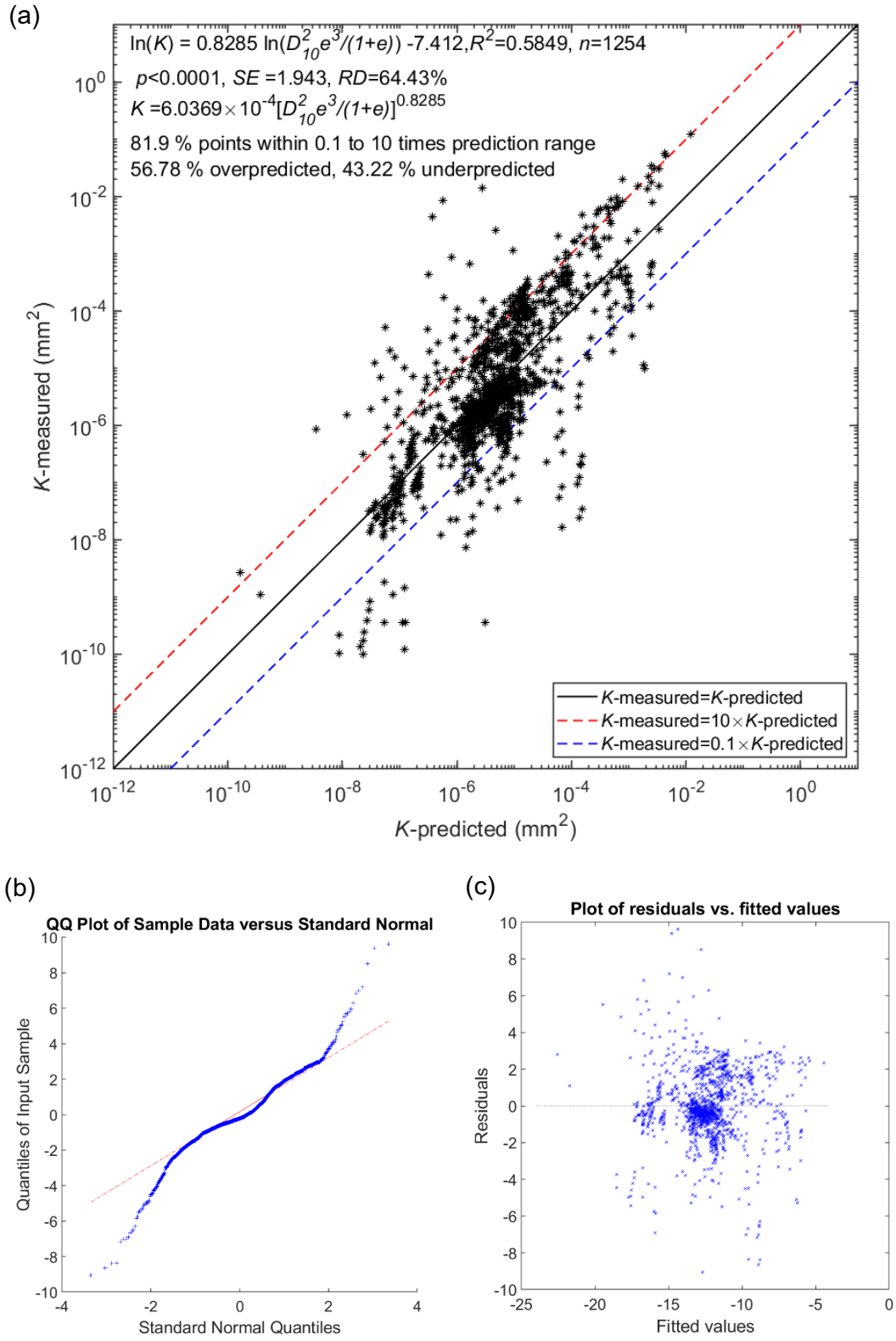

Figure S3. Regression result using a Chapuis (2004) style model: calibrated using the full database (plots adapted from Feng 2022)

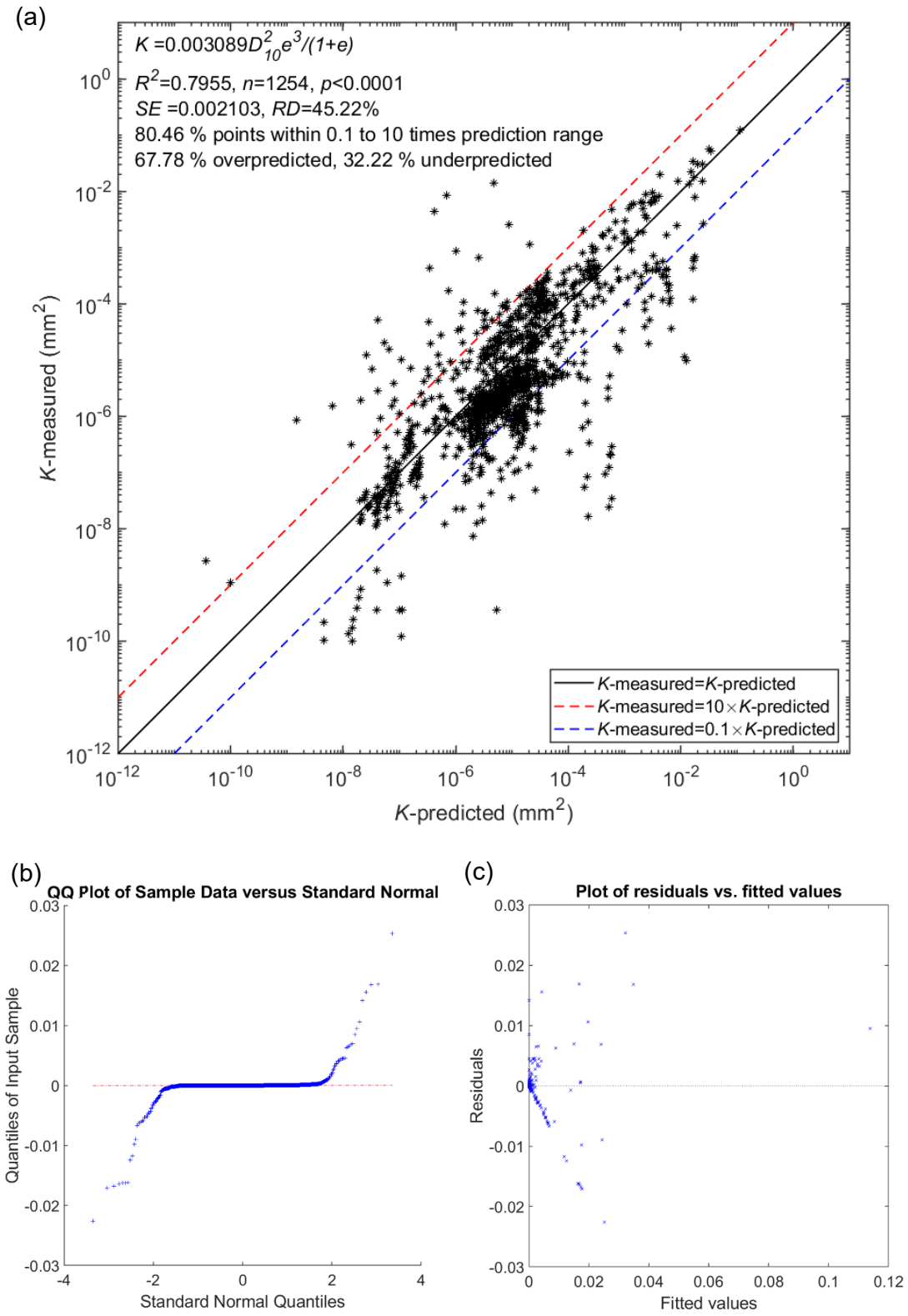

Figure S4. Regression result using a Taylor (1948) style model: calibrated using the full database (plots adapted from Feng 2022)

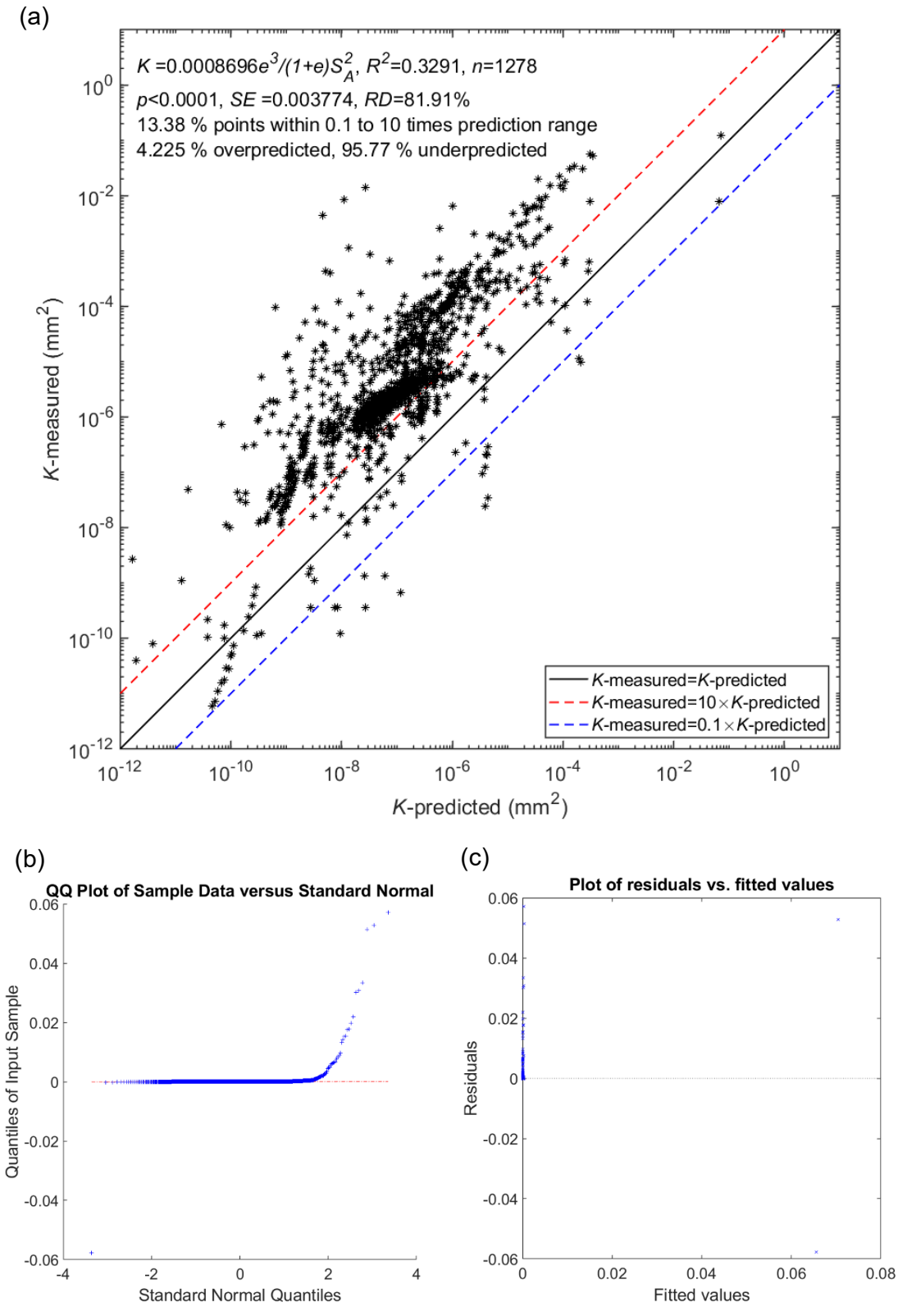

Figure S5. Regression result using a 'Kozeny-Carman' style model (Kozeny, 1927; Carman 1937, 1939): calibrated using the full database (plots adapted from Feng 2022)

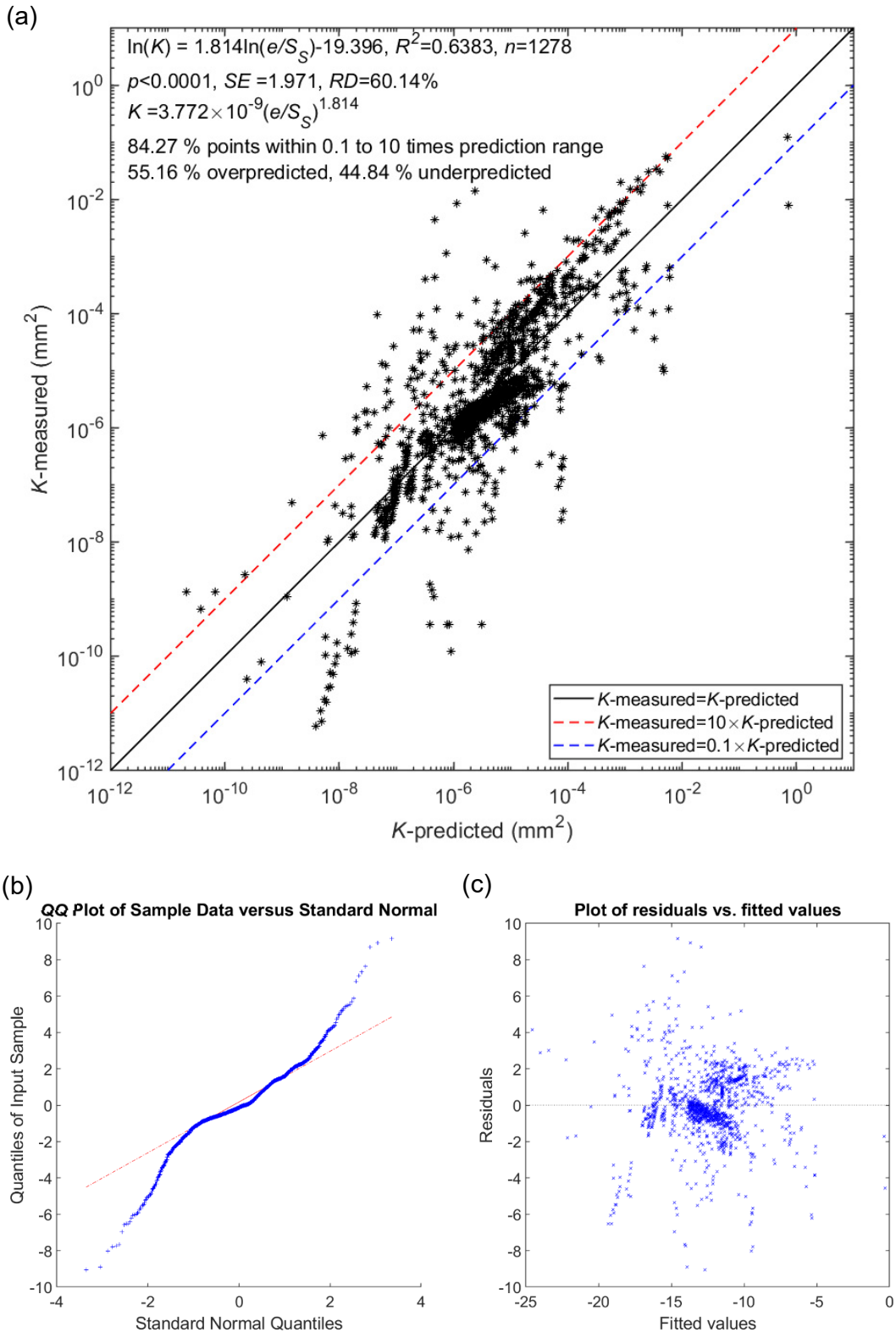

Figure S6. Regression result using a Feng & Vardanega (2019) style model: calibrated using the full database (plots adapted from Feng 2022)

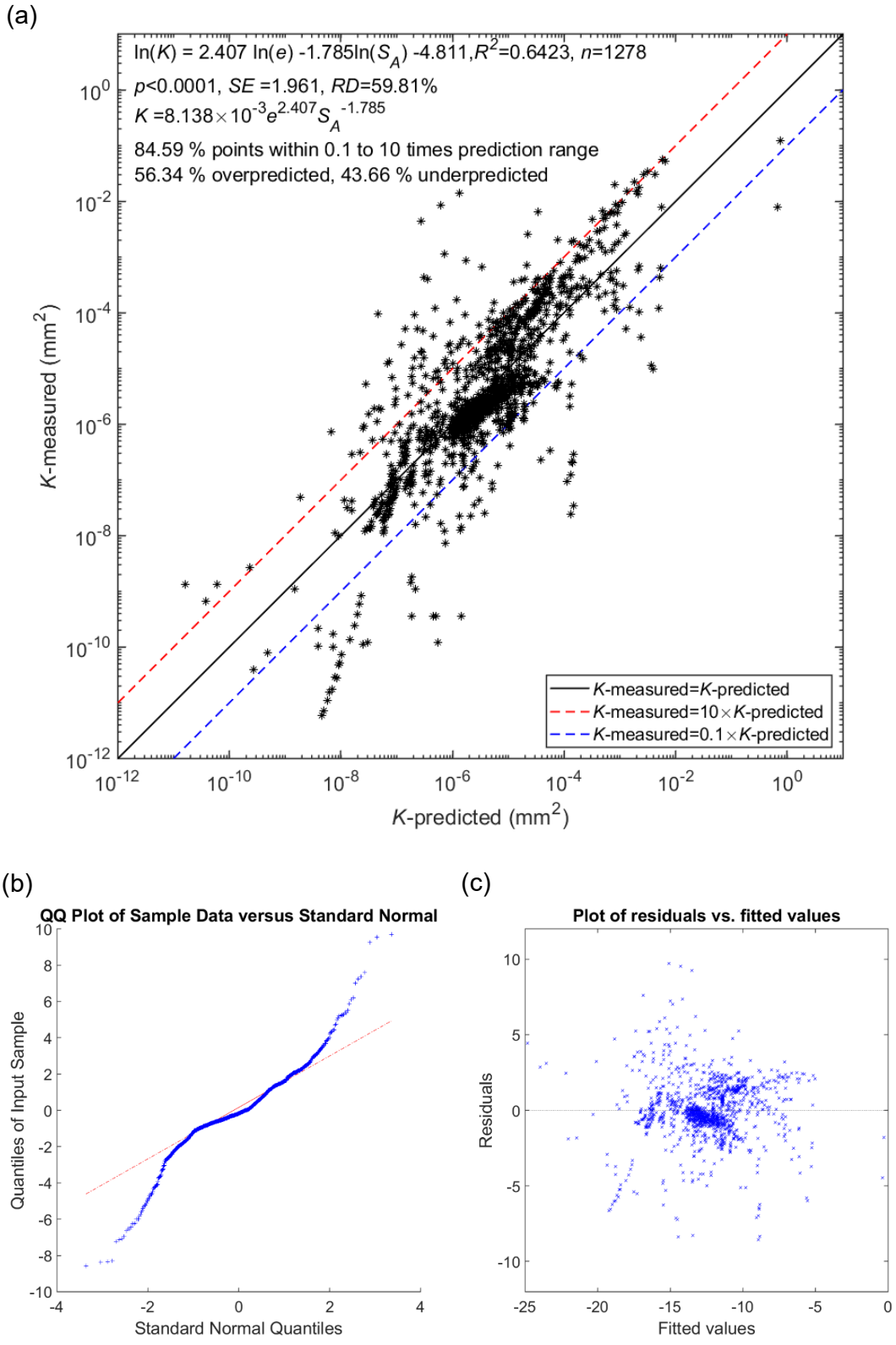

Figure S7. Regression result using a hydraulic radius style model (with a variable exponent on S_A): calibrated using the full database

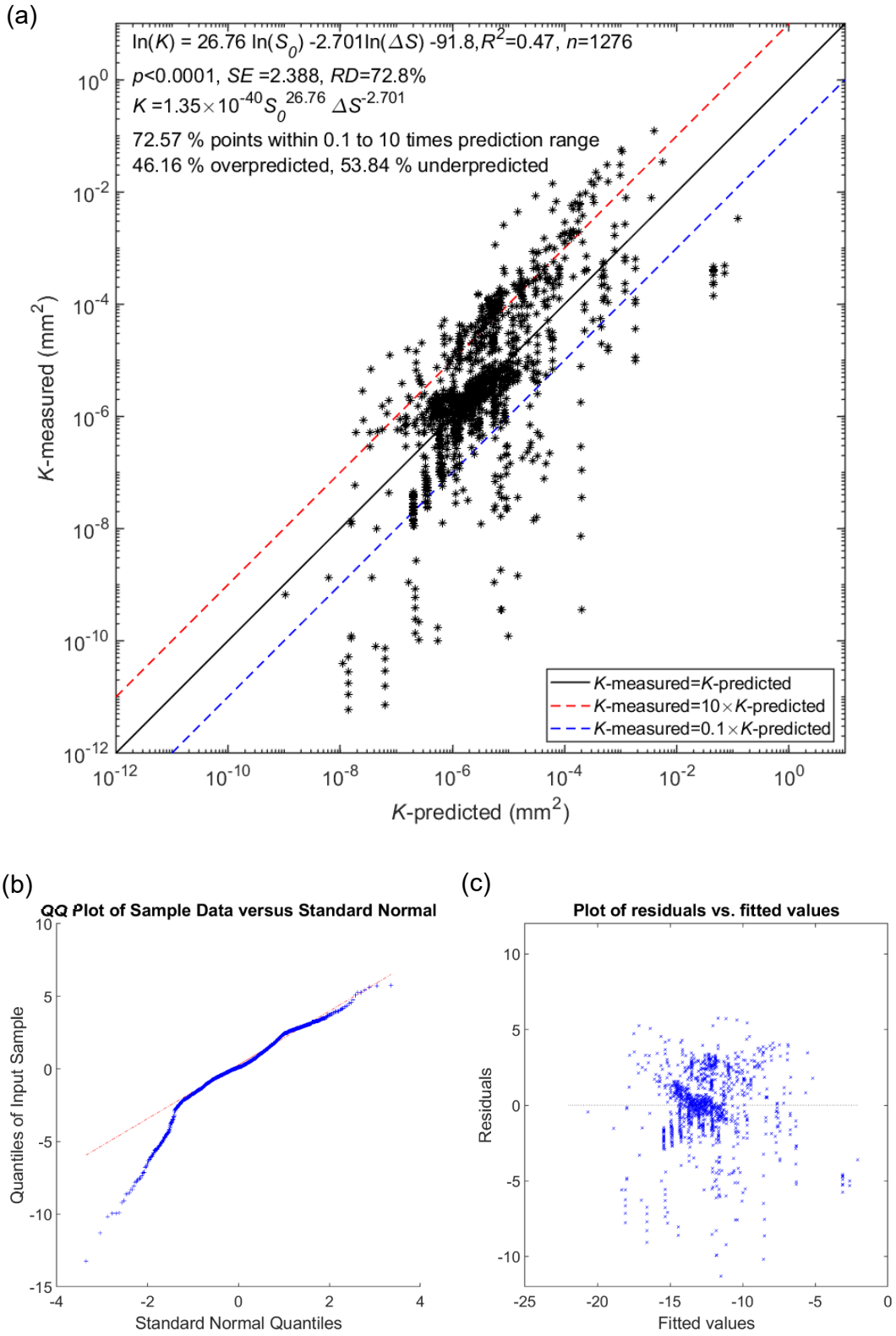

Figure S8. Regression result using a Feng et al. (2019) modified style model: calibrated using the full database (plots adapted from Feng 2022)

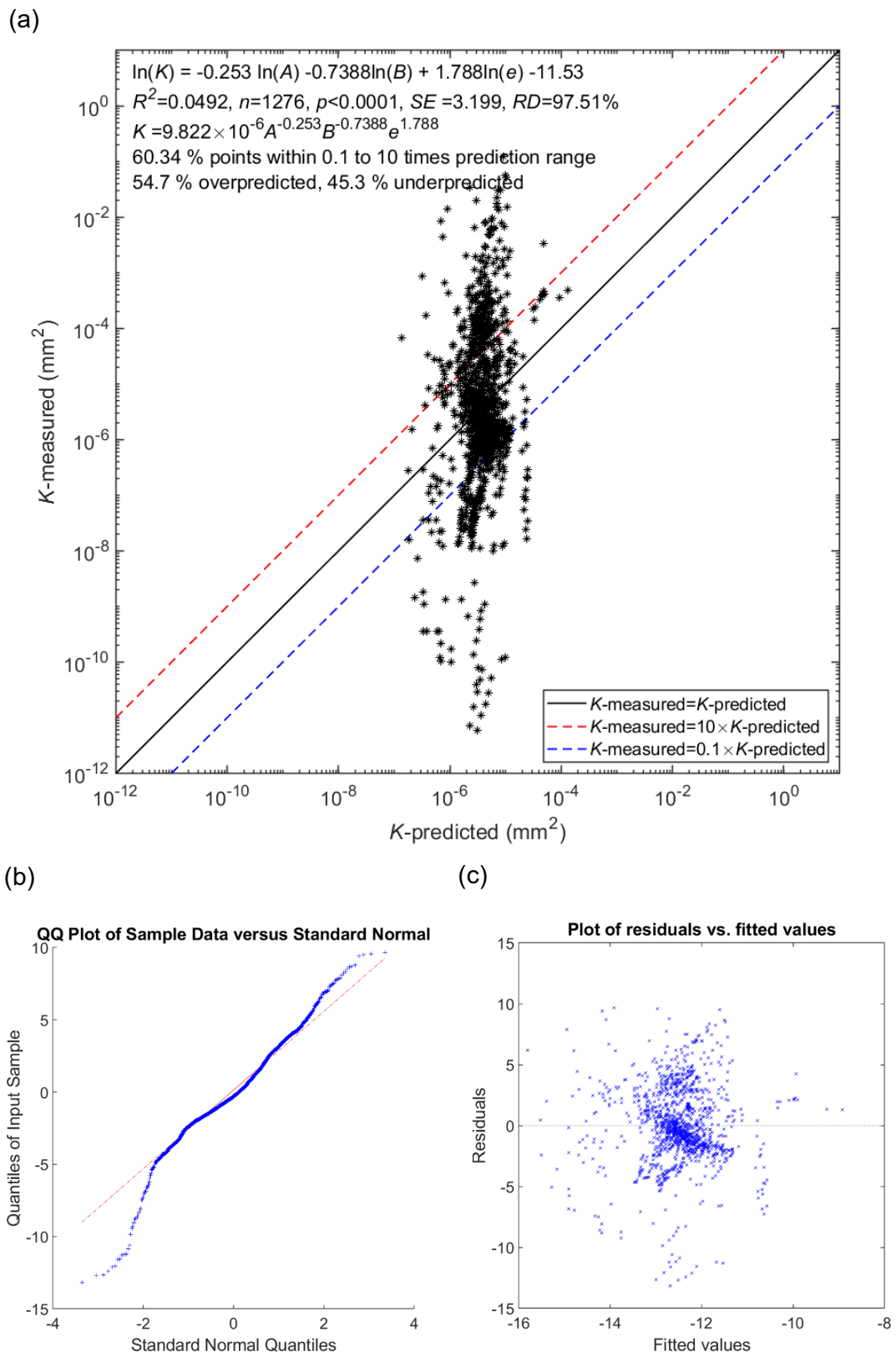

Figure S9. Regression result using a Feng et al. (2020) style model: calibrated using the full database (plots adapted from Feng 2022)

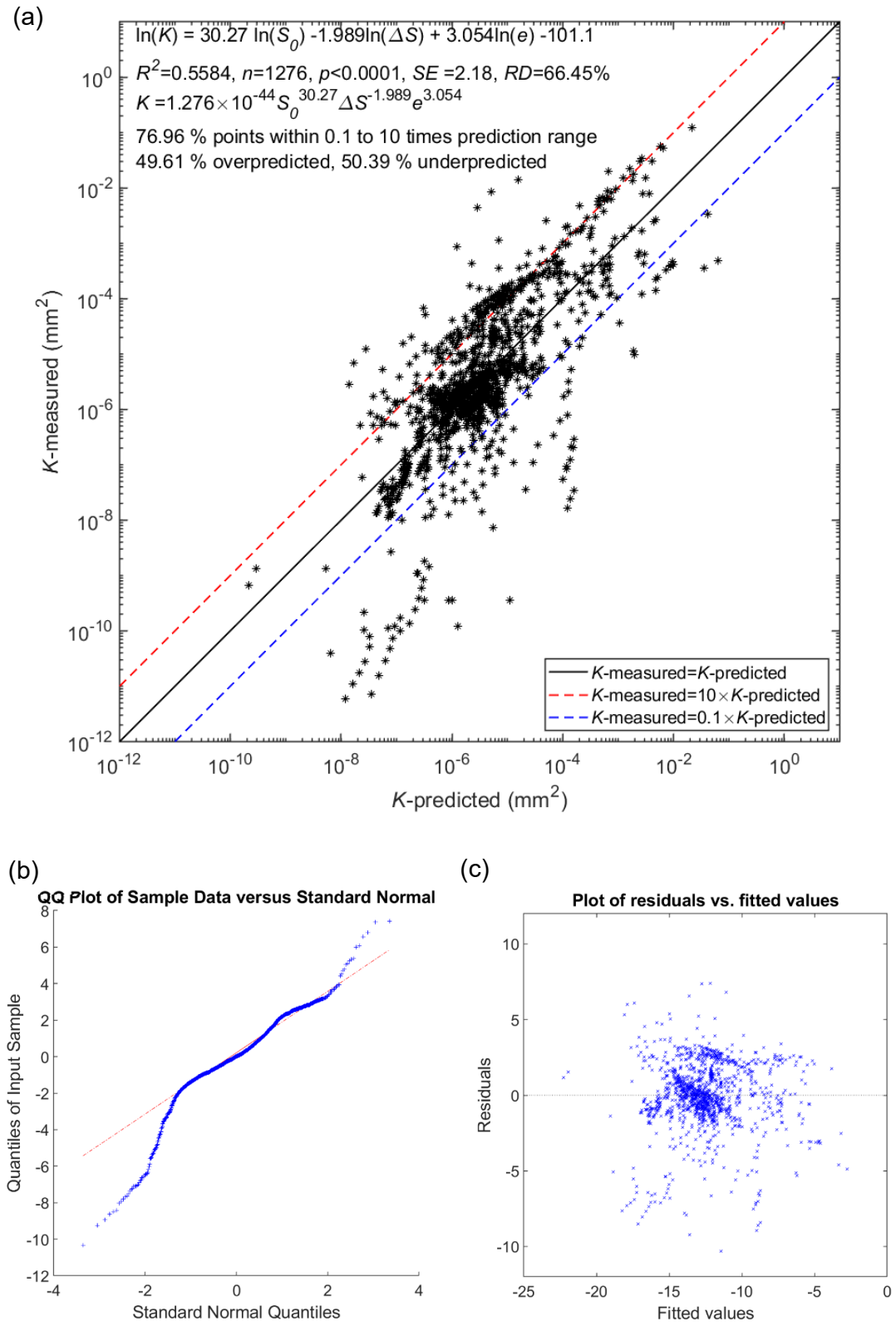

Figure S10. Regression result based on a Feng et al. (2020) modified style model: calibrated using the full database (plots adapted from Feng 2022)

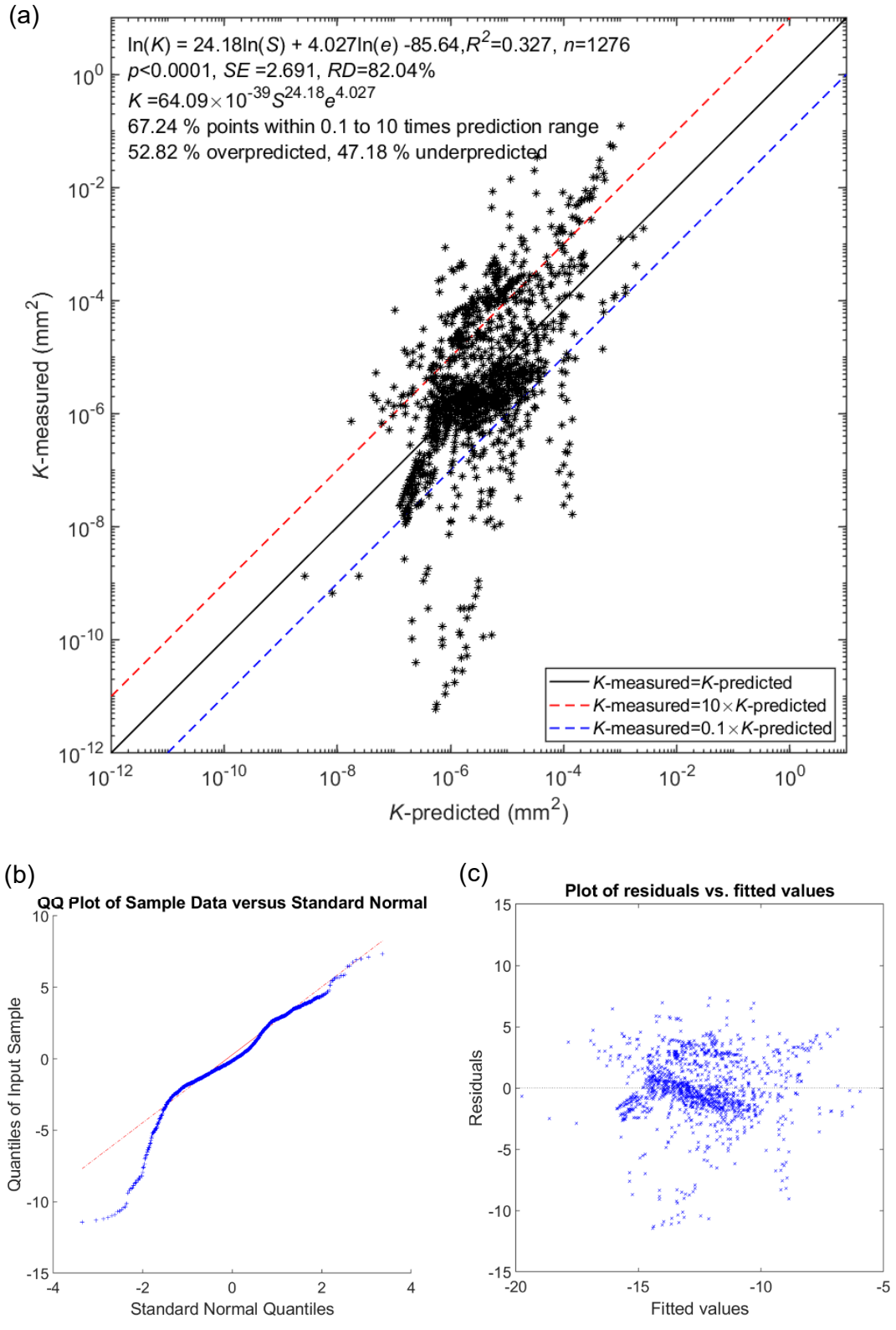

Figure S11. Regression result using a Feng et al. (2021) style model: calibrated based on the full database (plots adapted from Feng 2022)

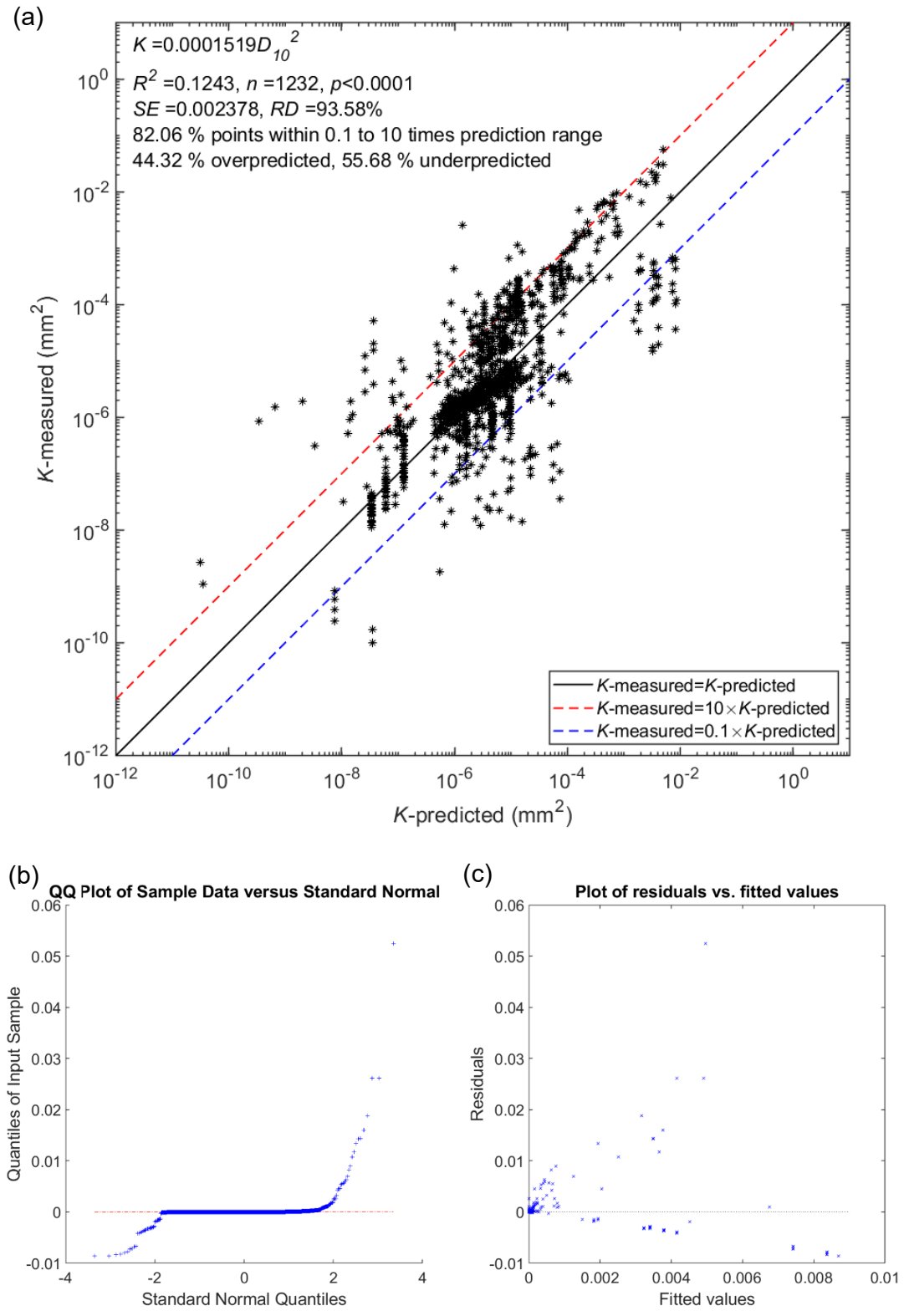

Figure S12. Regression result using a Hazen (1893, 1895, 1911) style model: calibrated using the cleaned database with global outliers removed (plots adapted from Feng 2022)

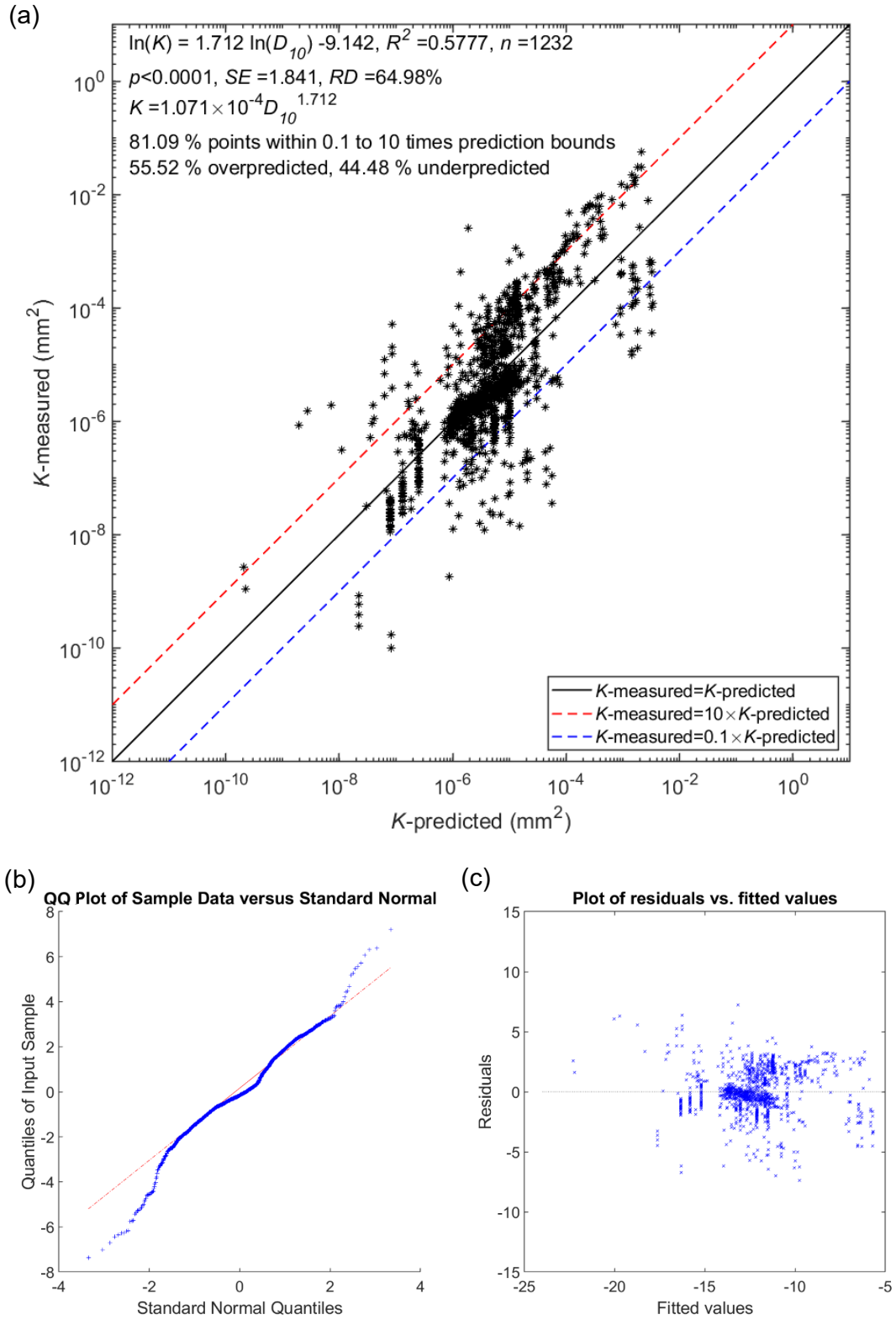

Figure S13. Regression result using a Shepherd (1989) style model: calibrated using the cleaned database with global outliers removed (plots adapted from Feng 2022)

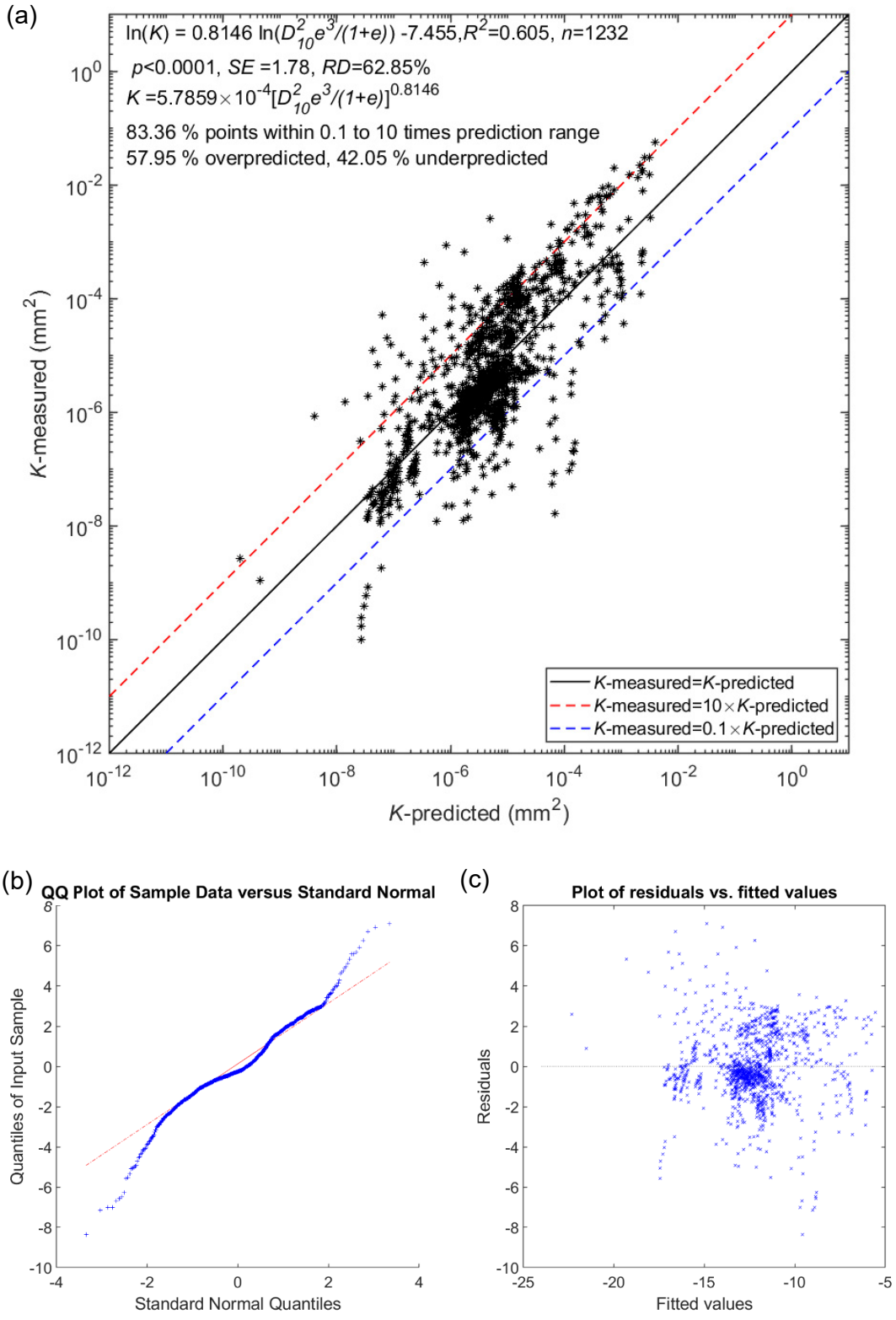

Figure S14. Regression result using a Chapuis (2004) style model: calibrated using the cleaned database with global outliers removed (plots adapted from Feng 2022)

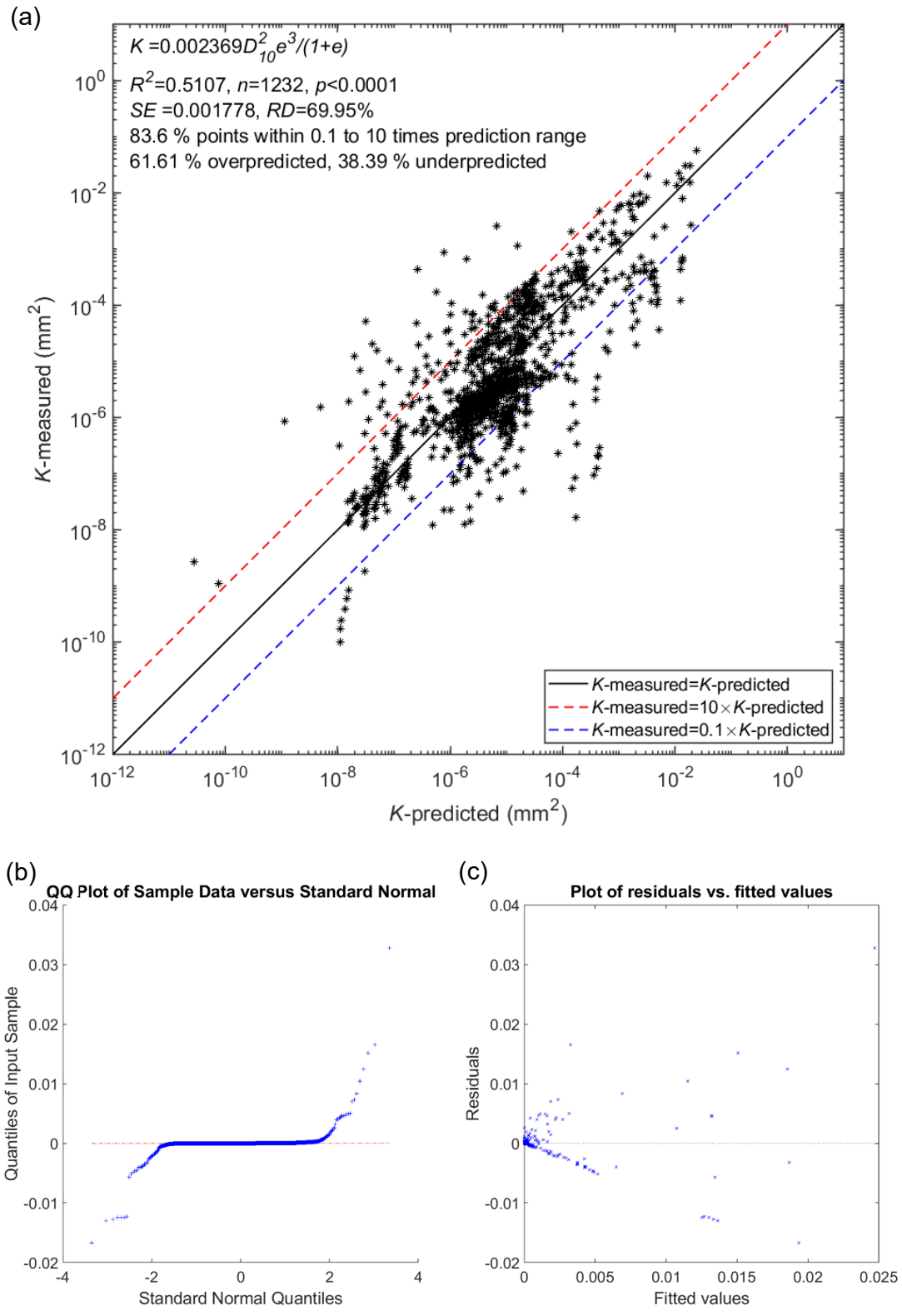

Figure S15. Regression result using a Taylor (1948) style model: calibrated using the cleaned database with global outliers removed (plots adapted from Feng 2022)

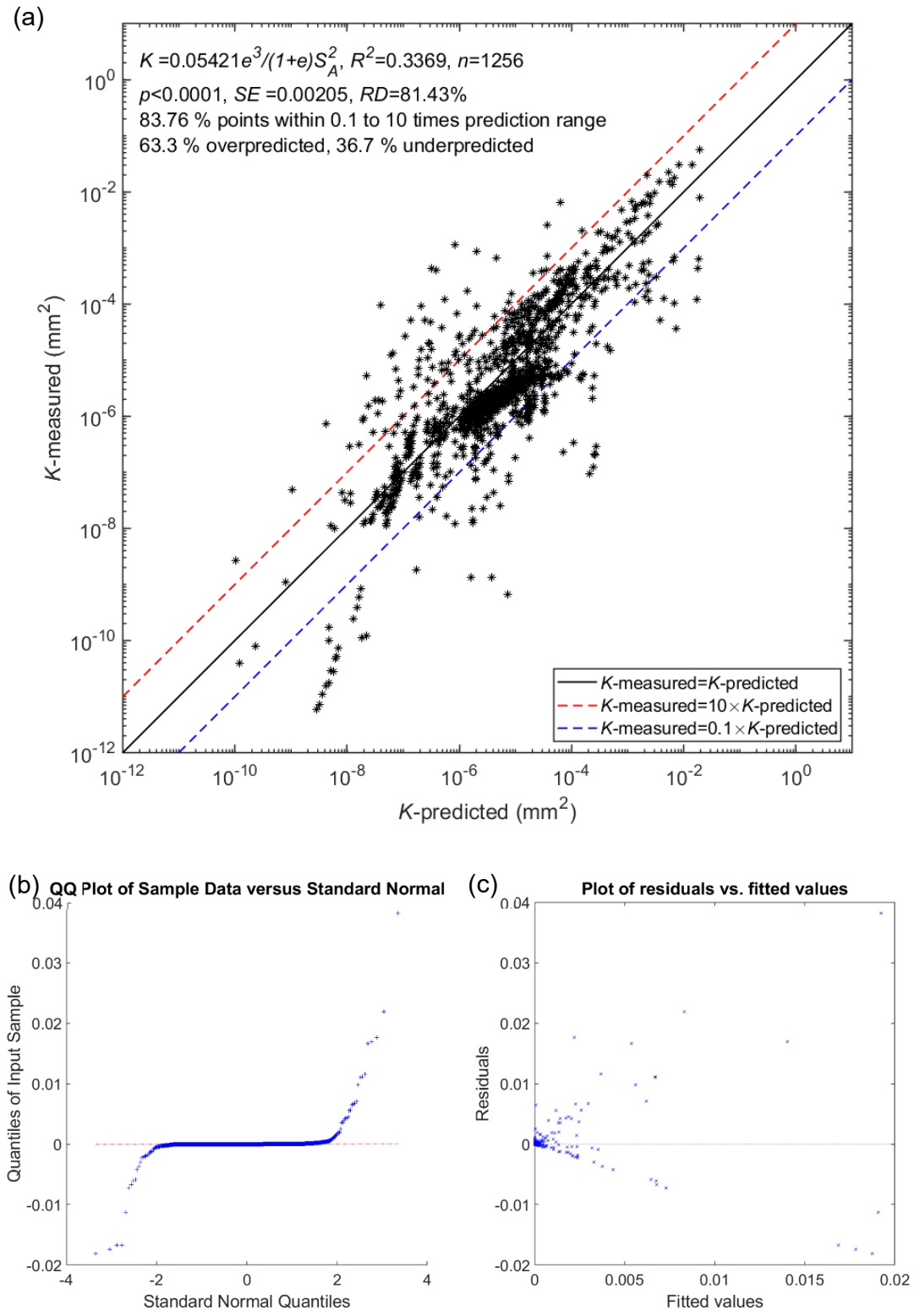

Figure S16. Regression result using a 'Kozeny-Carman' style model (Kozeny, 1927; Carman 1937, 1939): calibrated using the cleaned database with global outliers removed (plots adapted from Feng 2022)

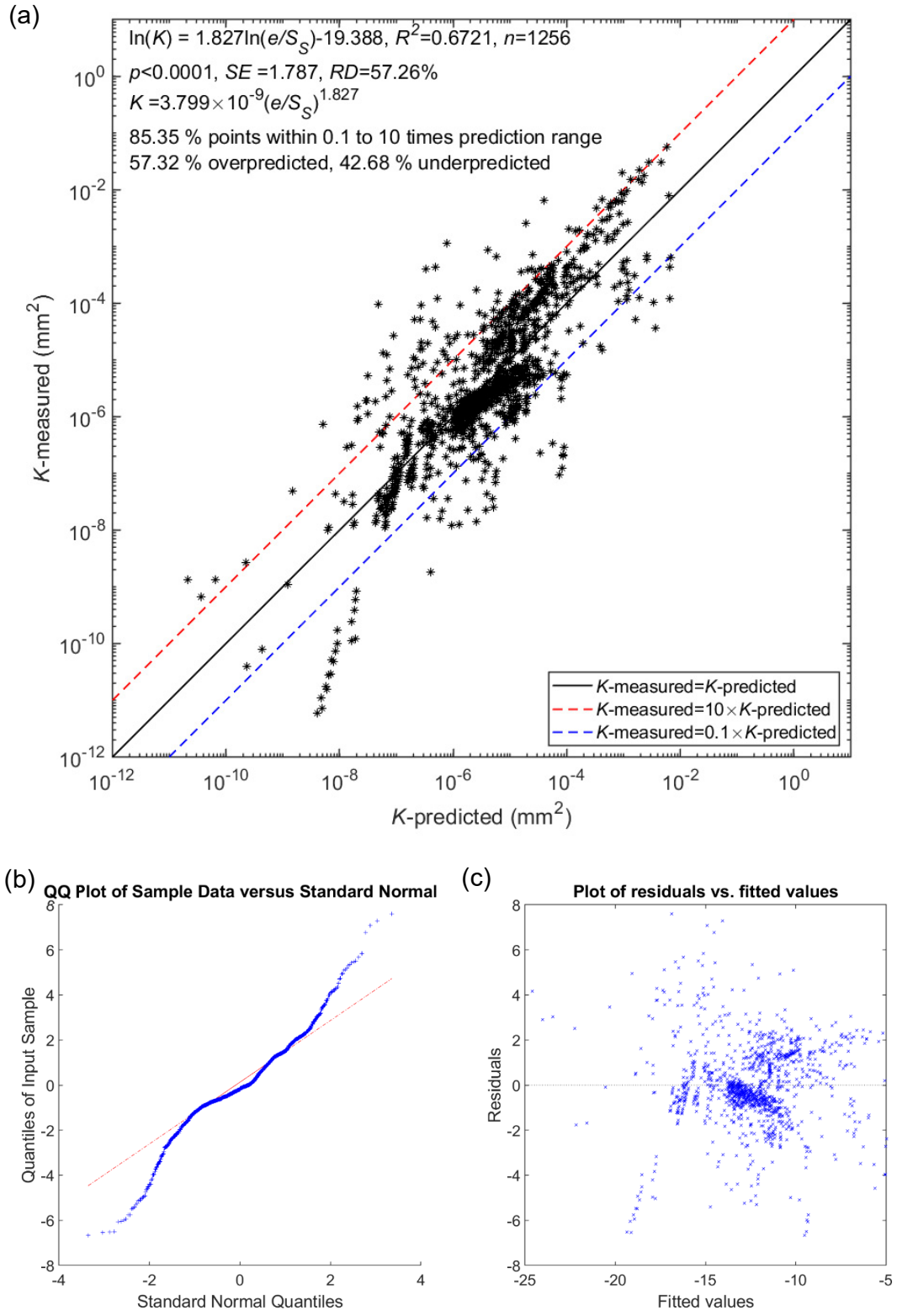

Figure S17. Regression result using a Feng & Vardanega (2019) style model: calibrated using the cleaned database with global outliers removed (plots adapted from Feng 2022)

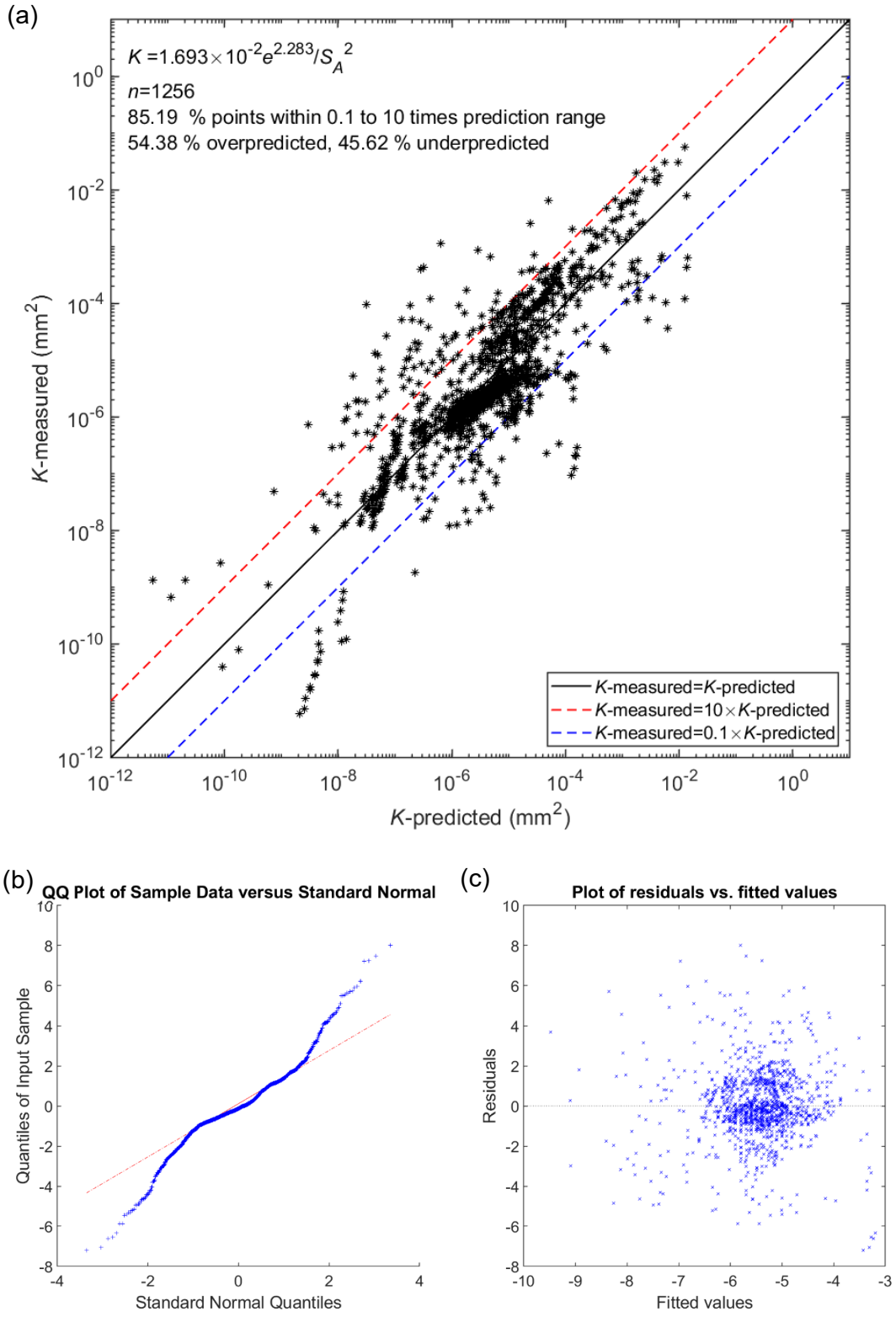

Figure S18. Regression result using a hydraulic radius style model (this study): calibrated using the cleaned database with global outliers removed (plots adapted from Feng 2022)

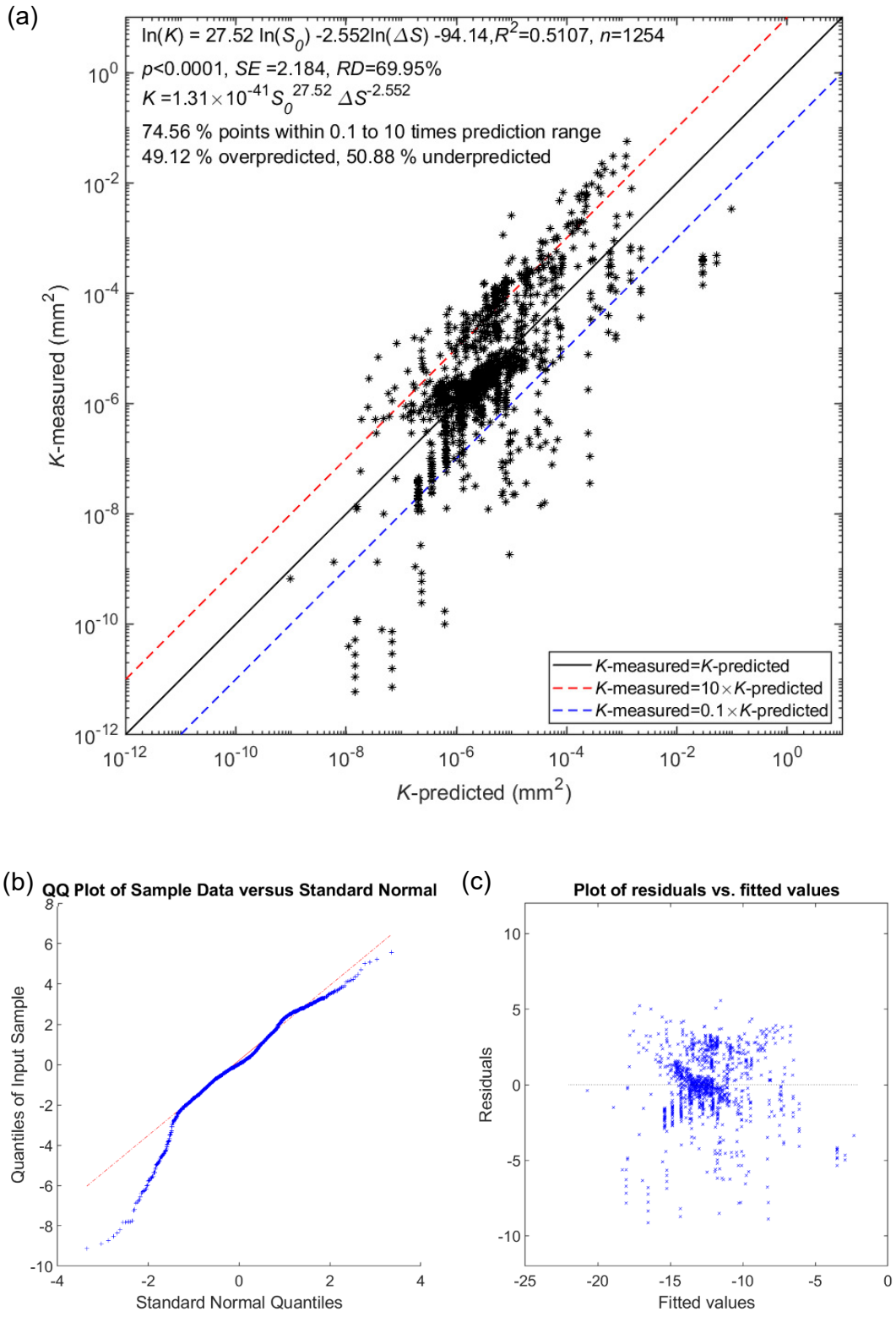

Figure S19. Regression result using a Feng et al. (2019) modified style model: calibrated using the cleaned database with global outliers removed (plots adapted from Feng 2022)

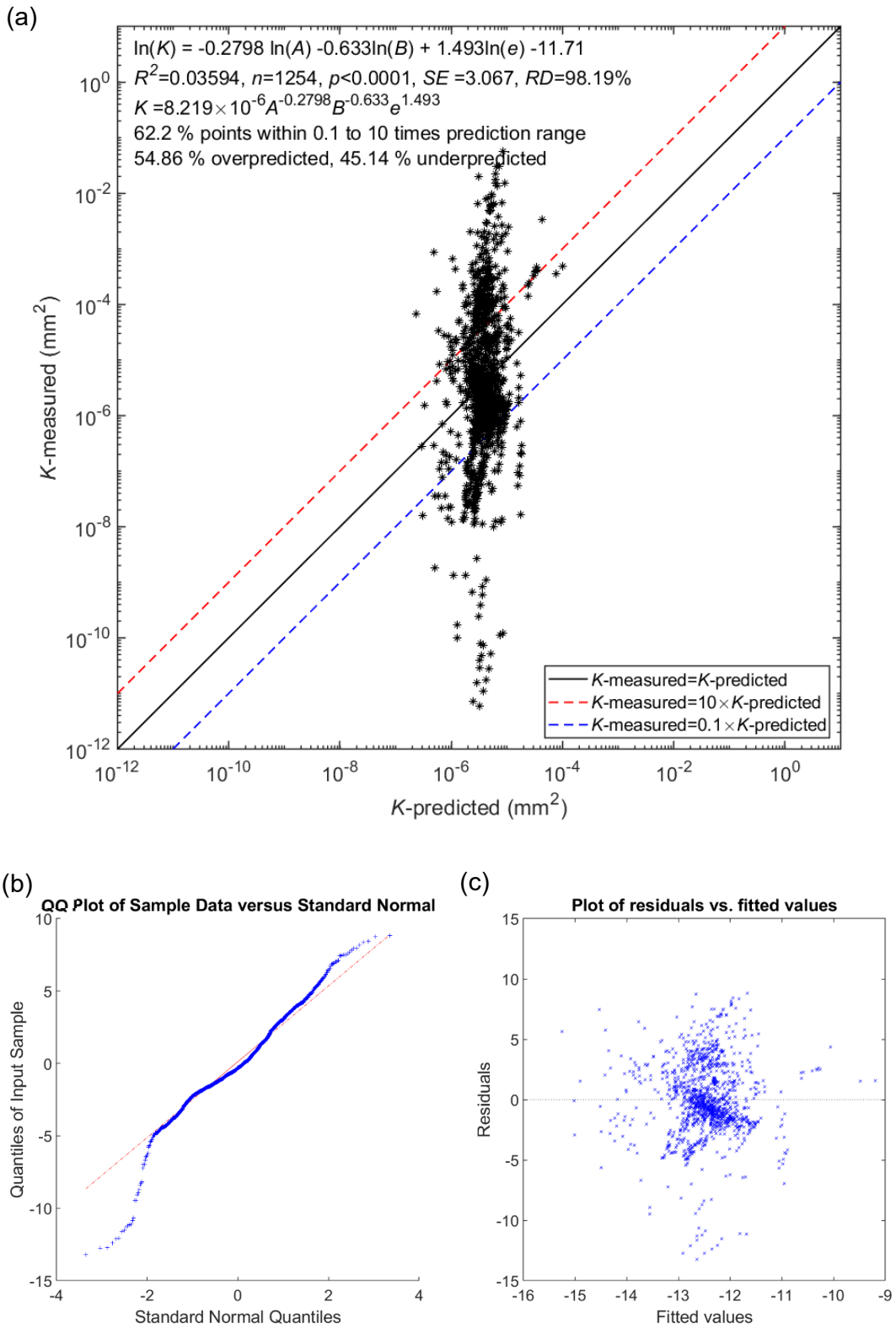

Figure S20. Regression result using a Feng et al. (2020) style model: calibrated using the cleaned database with global outliers removed (plots adapted from Feng 2022)

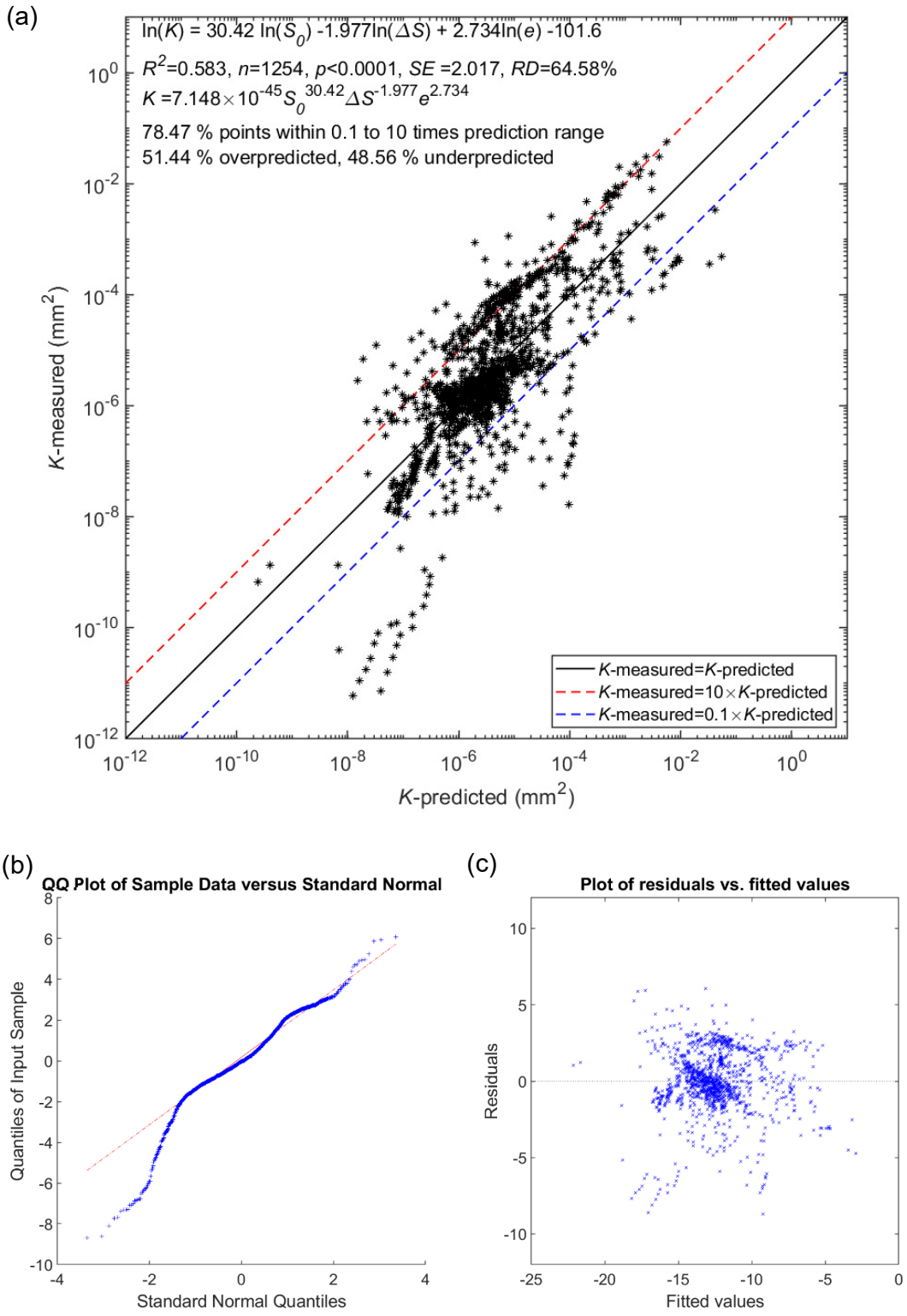

Figure S21. Regression result based on a Feng et al. (2020) modified style model: calibrated using the cleaned database with global outliers removed (plots adapted from Feng 2022)

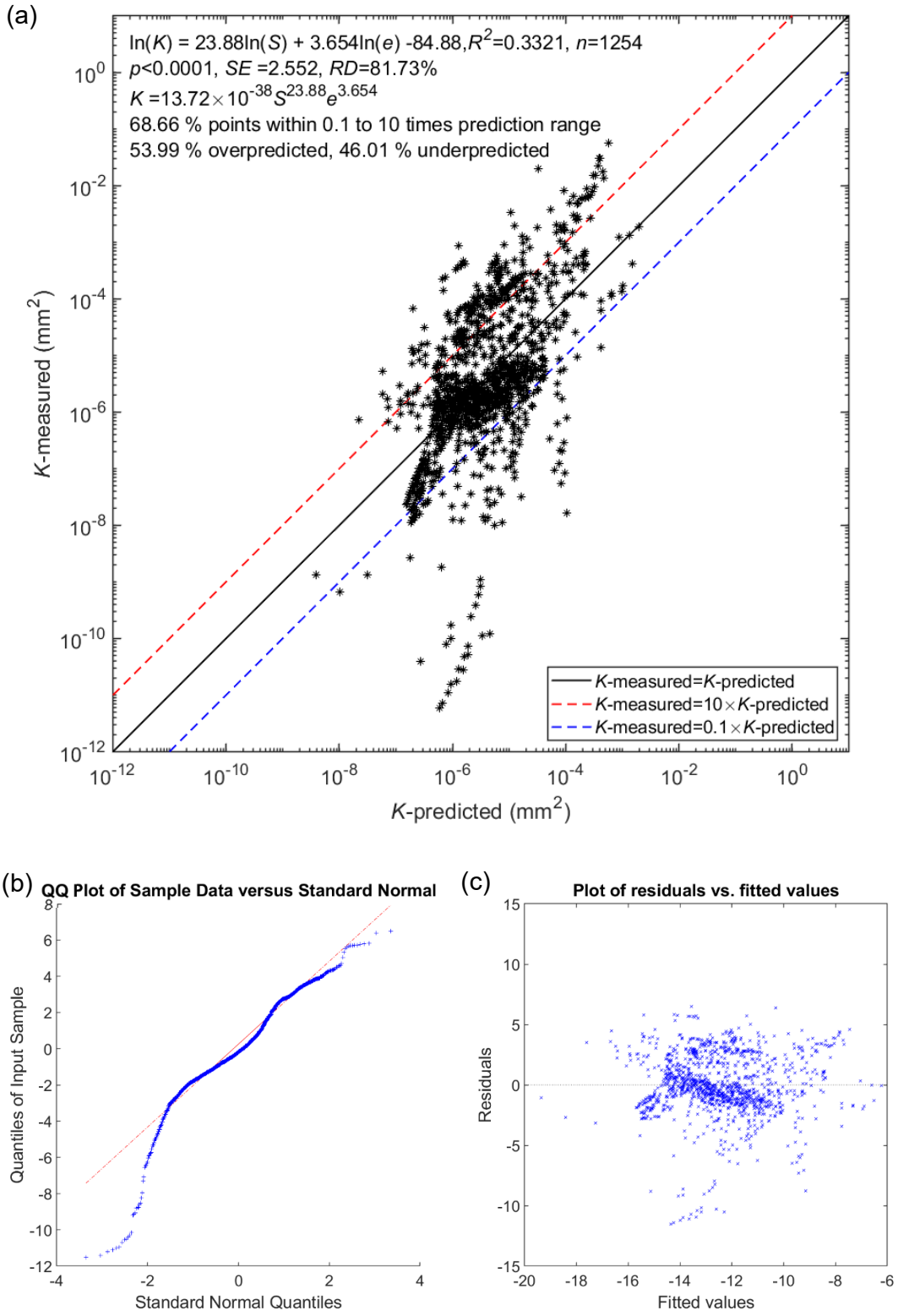

Figure S22. Regression result using a Feng et al. (2020) style model: calibrated using the cleaned database with global outliers removed (plots adapted from Feng 2022)

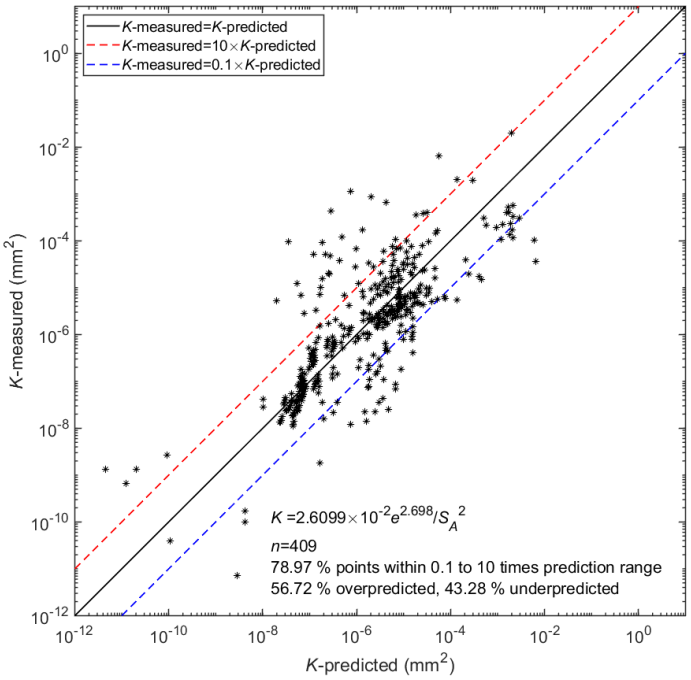

Figure S23. *k*-measured versus *k*-predicted for data subset '*e*< 0.5' (plot adapted from Feng 2022)

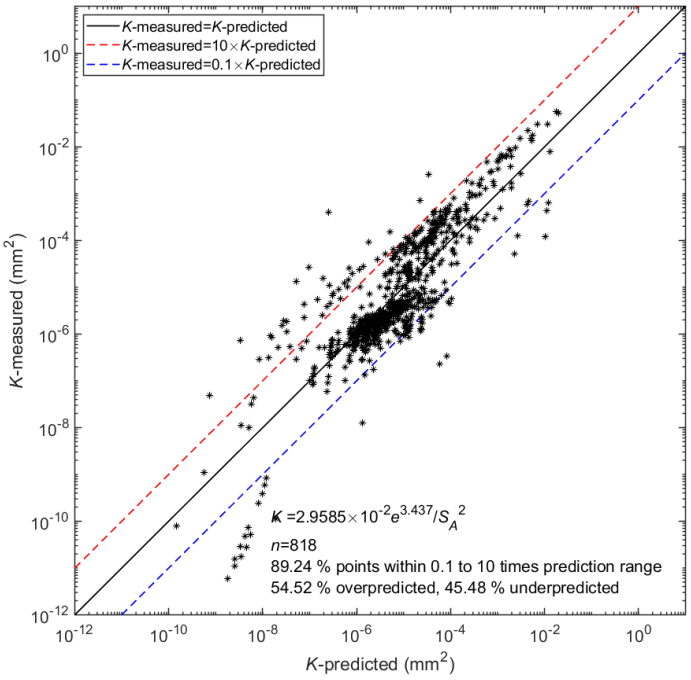

Figure S24. *k*-measured versus *k*-predicted for data subset '0.5≤ *e*<1' (plot adapted from Feng 2022)

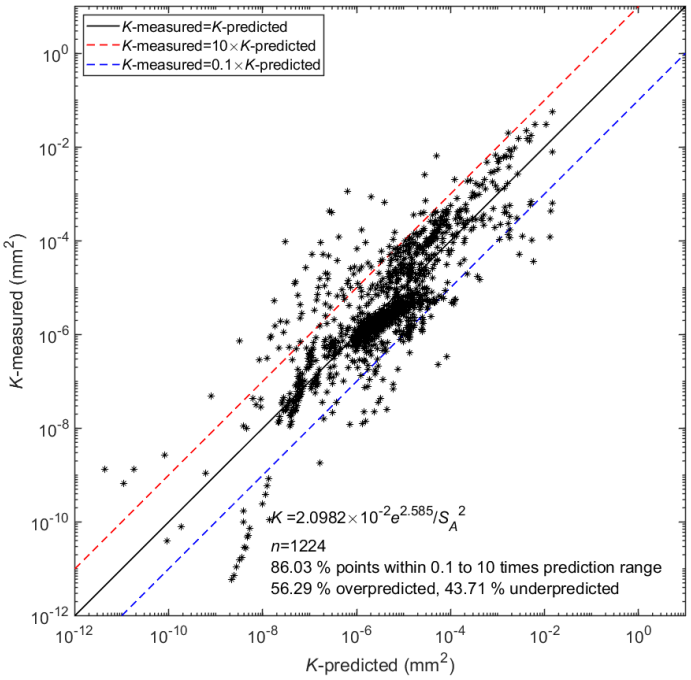

Figure S25. *k*-measured versus *k*-predicted for data subset '*e*< 1' (plot adapted from Feng 2022)

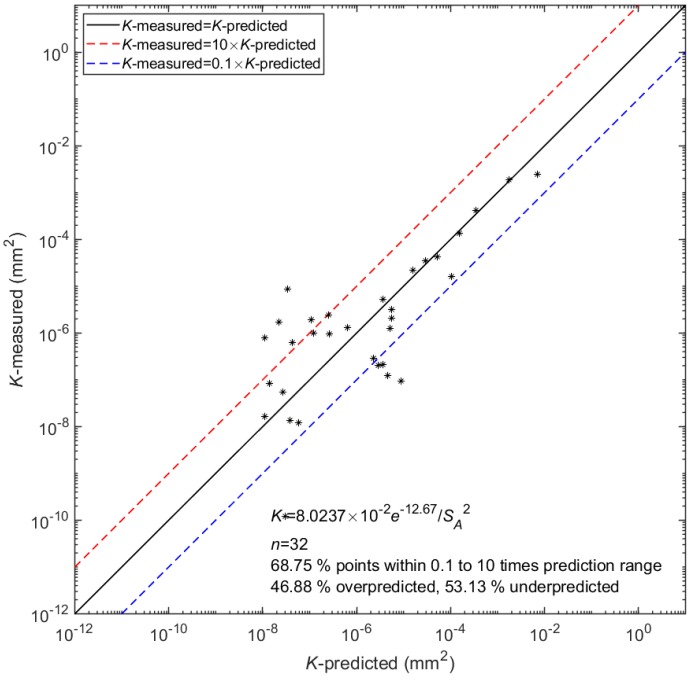

Figure S26. *k*-measured versus *k*-predicted for data subset '*e*≥ 1' (plot adapted from Feng 2022)

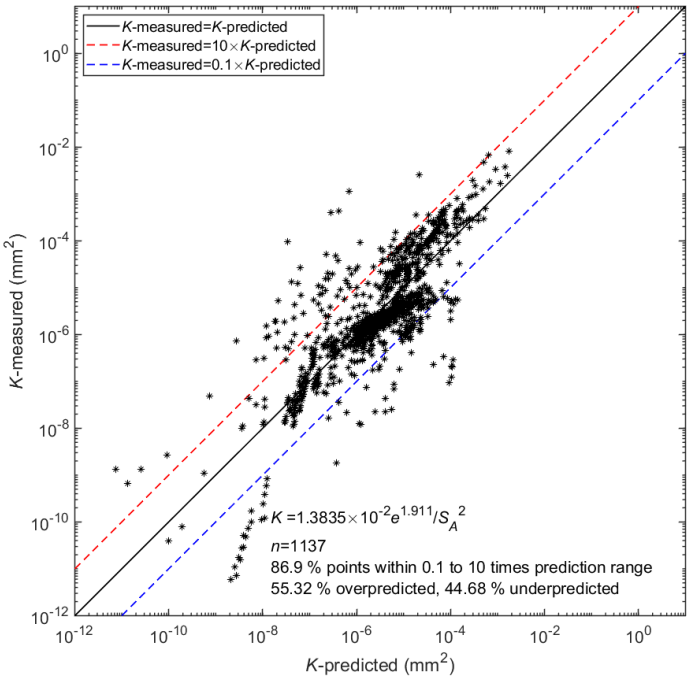

Figure S27. *k*-measured versus *k*-predicted for data subset 'sand' (plot adapted from Feng 2022)

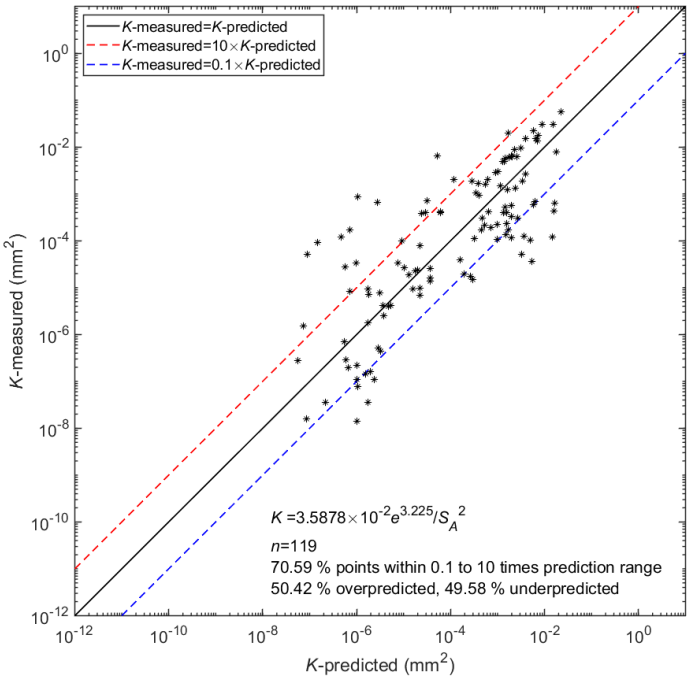

Figure S28. *k*-measured versus *k*-predicted for data subset 'gravel' (plot adapted from Feng 2022)

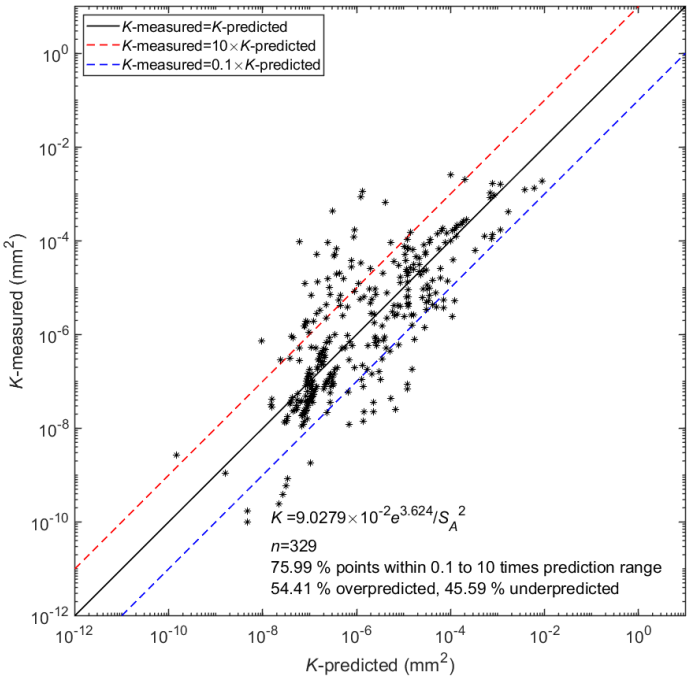

Figure S29. *k*-measured versus *k*-predicted for data subset '$C_U \geq 6$' (plot adapted from Feng 2022)

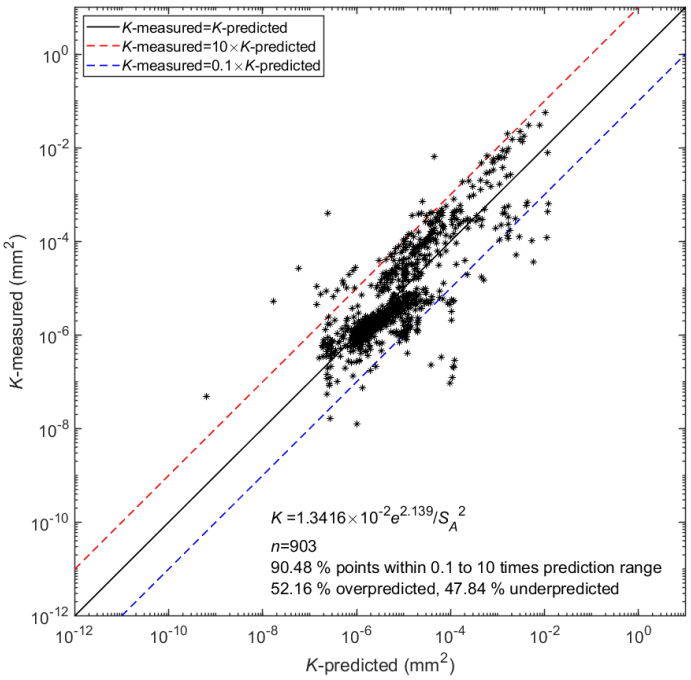

Figure S30. *k*-measured versus *k*-predicted for data subset '$C_U < 6$' (plot adapted from Feng 2022)

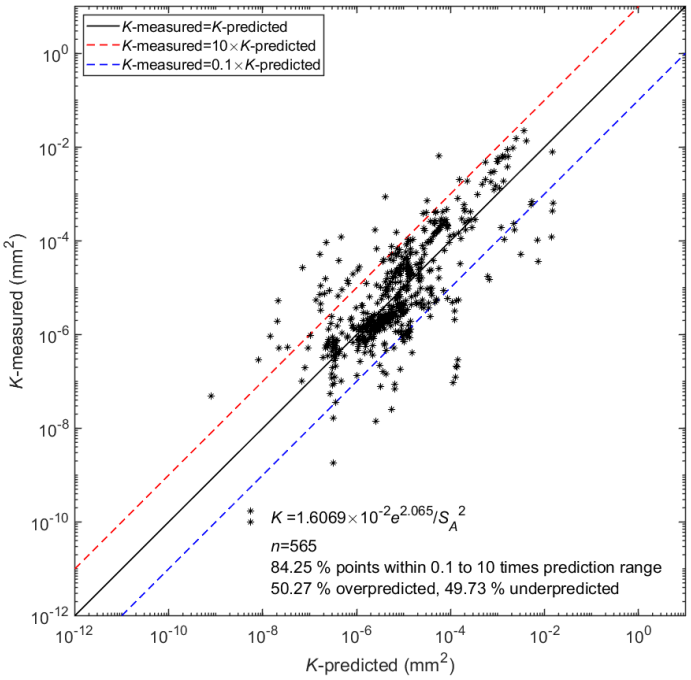

Figure S31. *k*-measured versus *k*-predicted for data subset '1≤ C_Z≤ 3' (plot adapted from Feng 2022)

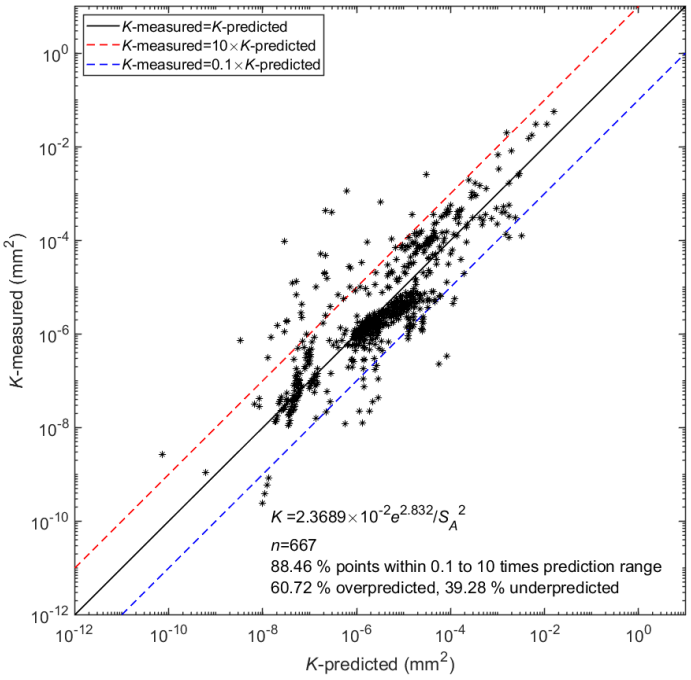

Figure S32. *k*-measured versus *k*-predicted for data subset '1> C_Z or C_Z>3' (plot adapted from Feng 2022)

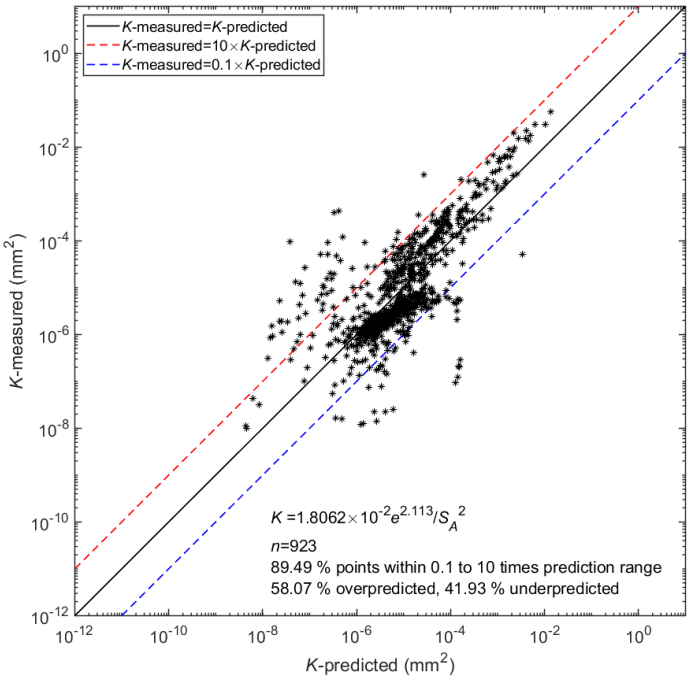

Figure S33. *k*-measured versus *k*-predicted for data subset 'constant head test' (plot adapted from Feng 2022)

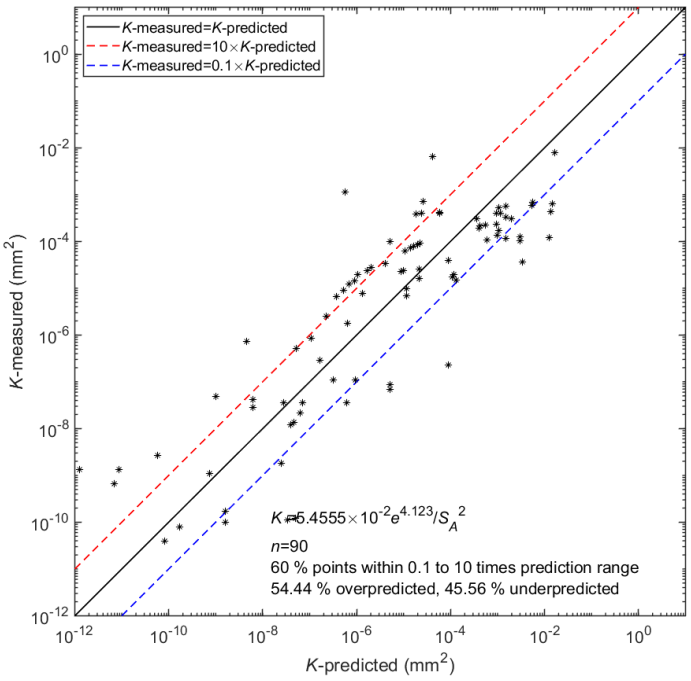

Figure S34. *k*-measured versus *k*-predicted for data subset 'falling head test' (plot adapted from Feng 2022)

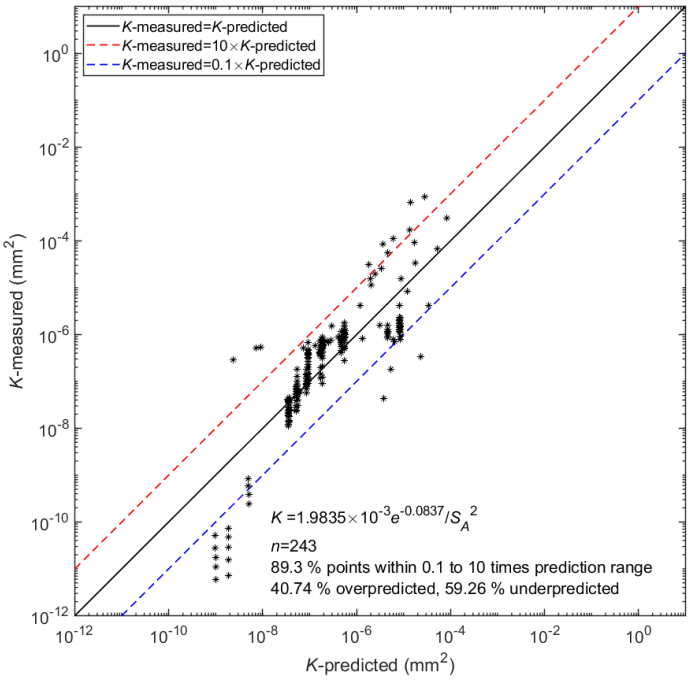

Figure S35. *k*-measured versus *k*-predicted for data subset 'other test method' (plot adapted from Feng 2022)

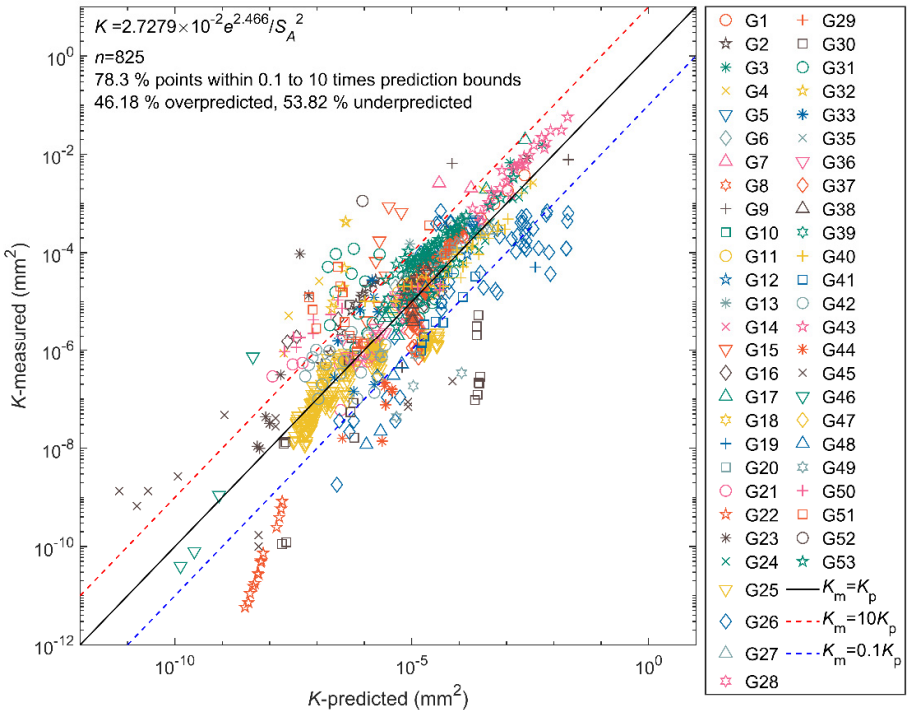

Figure S36: Calibration of Eq. 4 with G01-G53 excluding G34 (see Table 9)

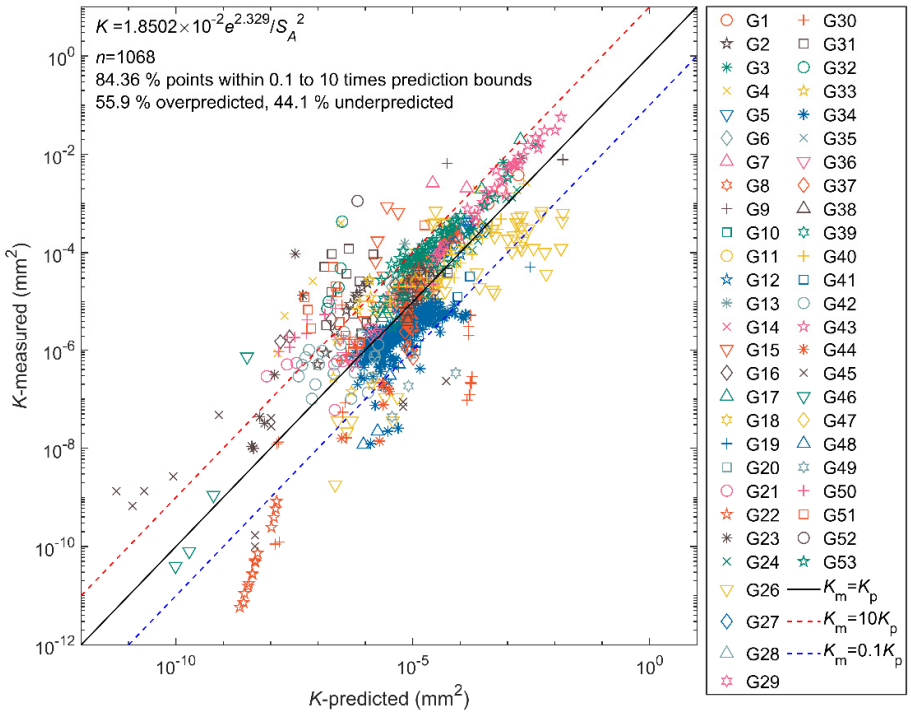

Figure S37: Calibration of Eq. 4 with G01-G53 excluding G25 (see Table 9)

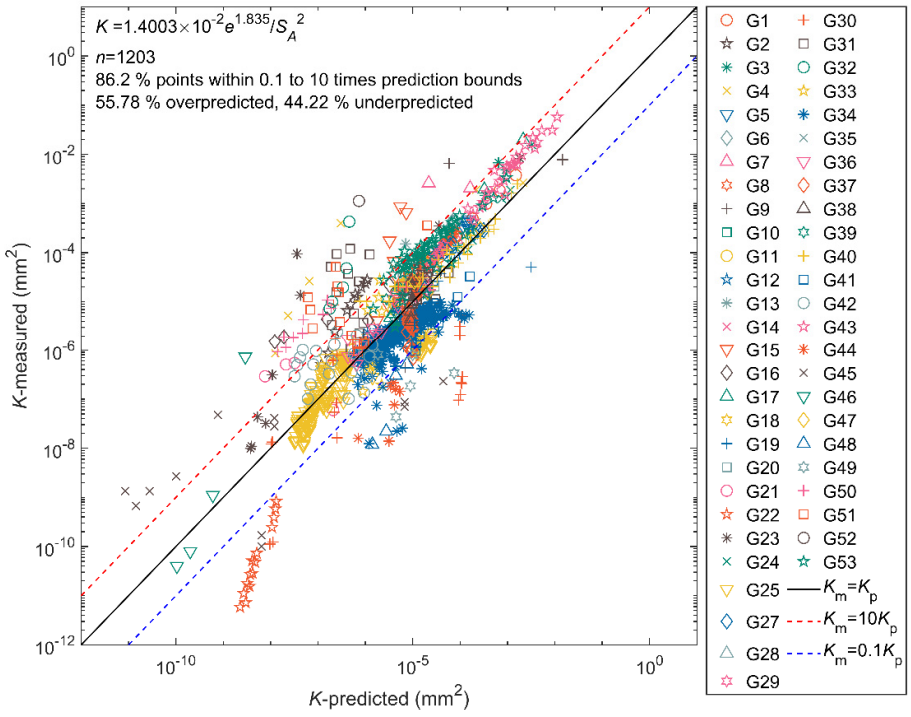

Figure S38: Calibration of Eq. 4 with G01-G53 excluding G26 (see Table 9)

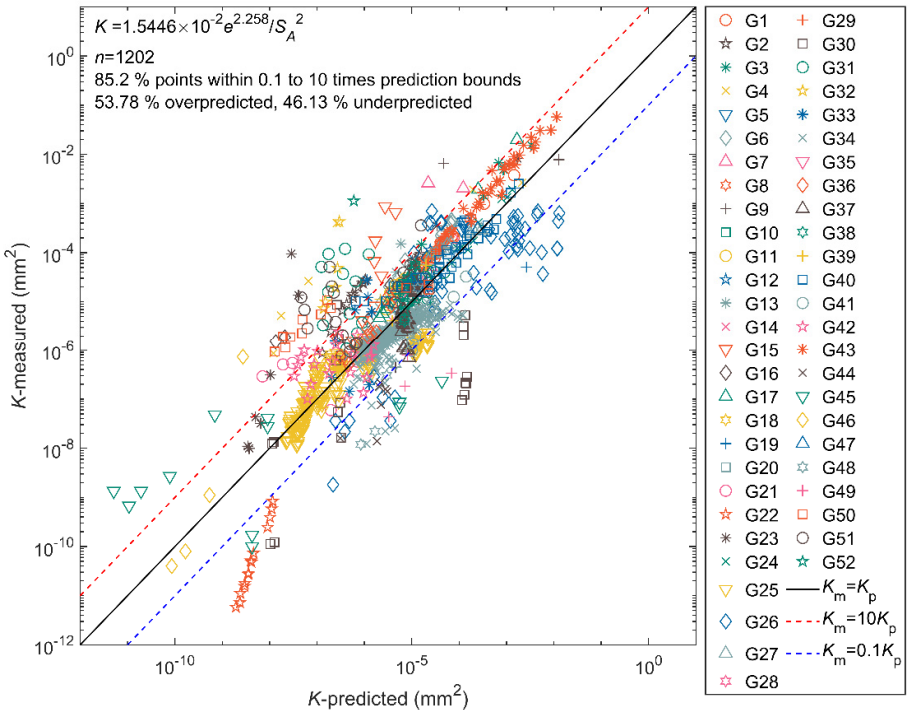

Figure S39: Calibration of Eq. 4 with G01-G53 excluding G53 (see Table 9)

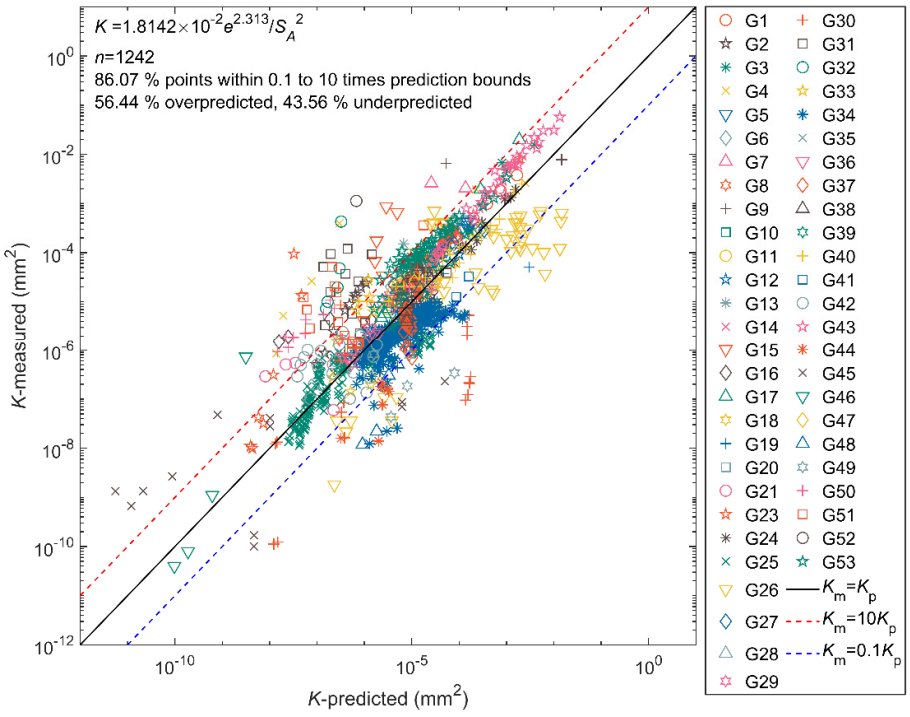

Figure S40: Calibration of Eq. 4 with G01-G53 excluding G22 (see Table 9)

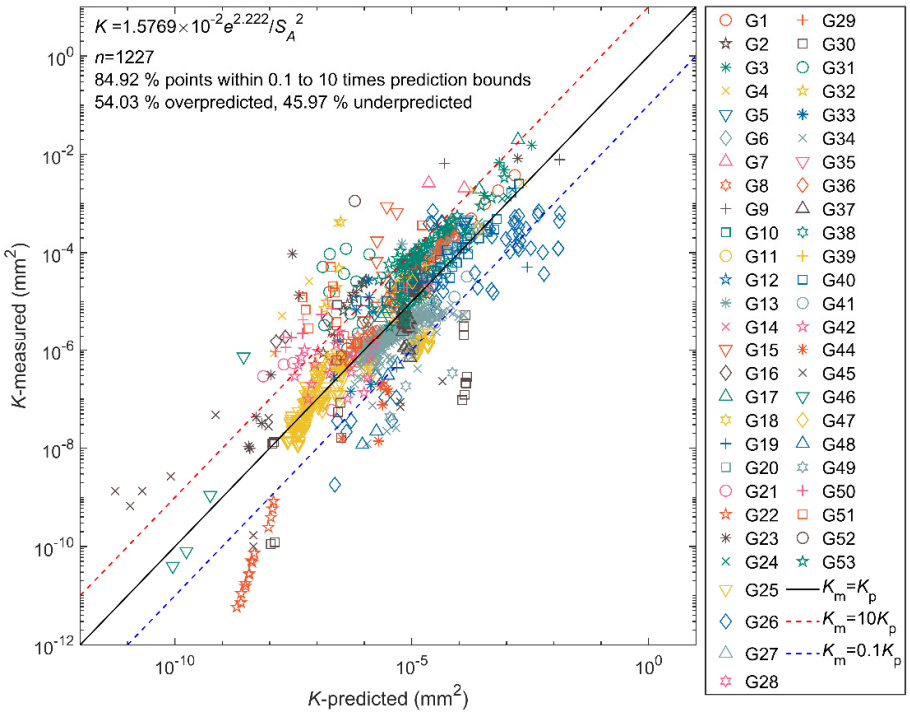

Figure S41: Calibration of Eq. 4 with G01-G53 excluding G43 (see Table 9)

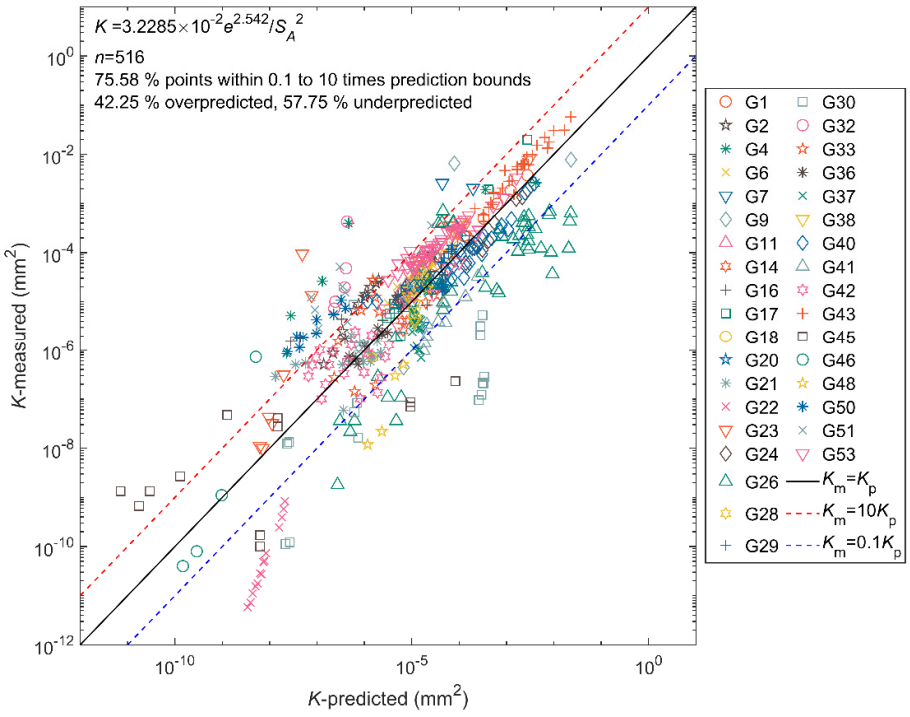

Figure S42: Calibration of Eq. 4 with G01-G53 excluding sources with G_s unknown

REFERENCES

Carman, P.C. (1937). Fluid flow through granular beds. *Transaction Institution of Chemical Engineers*, **15:** 150–166.

Carman, P.C. (1939). Permeability of saturated sands, soils and clays. *The Journal of Agricultural Science*, **29(2):** 262-273. https://doi.org/10.1017/S0021859600051789

Chapuis, R.P. (2004). Predicting the saturated hydraulic conductivity of sand and gravel using effective diameter and void ratio. *Canadian Geotechnical Journal*, **41(5):** 787–795. https://doi.org/10.1139/t04-022

Feng, S. and Vardanega, P.J. (2019). Correlation of the Hydraulic Conductivity of Fine-Grained Soils with Water Content Ratio Using a Database. *Environmental Geotechnics*, **6(5):** 253-268. https://doi.org/10.1680/jenge.18.00166

Feng, S., Vardanega, P.J., Ibraim, E., Widyatmoko, I. and Ojum, C. (2019). Permeability assessment of some granular mixtures. *Géotechnique*, **69(7):** 646–654. https://doi.org/10.1680/jgeot.17.T.039

Feng, S., Vardanega, P.J., Ibraim, E., Widyatmoko, I., Ojum, C., O'Kelly, B.C. and Nogal, M. (2020). Discussion: Permeability assessment of some granular mixtures. *Géotechnique*, **70(9):** 845–847. https://doi.org/10.1680/jgeot.19.D.005

Feng, S., Vardanega, P.J., James, M. and Ibraim, E. (2021). Studying hydraulic conductivity of asphalt concrete using a database. *Transportation Engineering*, **3:**[100040]. https://doi.org/10.1016/j.treng.2020.100040

Feng S. (2022). Hydraulic Conductivity of Road Construction Materials: with a focus on freeze-thaw effects. *Ph.D. thesis*. University of Bristol, Bristol, UK.

Hazen, A. (1893). *Some physical properties of sand and gravels, 24th Annual Report*. Massachusetts State Board of Health, Wright & Potter Printing.

Hazen, A. (1895). *The filtration of public water supplies*. John Wiley & Sons, New York, NY.

Hazen, A. (1911). Discussion of "Dam on Sand Foundation" by A. C. Koenig. *Transactions of the American Society of Civil Engineers*, **73:** 199–203.

Kozeny, J. (1927). Über kapillare leitung des wassers im boden:(aufstieg, versickerung und anwendung auf die bewässerung) Hölder-Pichler-Tempsky (in German).

Shepherd, R.G. (1989). Correlations of Permeability and Grain Size. *Ground Water*, **27(5):** 633–638. https://doi.org/10.1111/j.1745-6584.1989.tb00476.x

Taylor, D.W. (1948). *Fundamentals of Soil Mechanics*. John Wiley & Sons Inc, New York, NY.